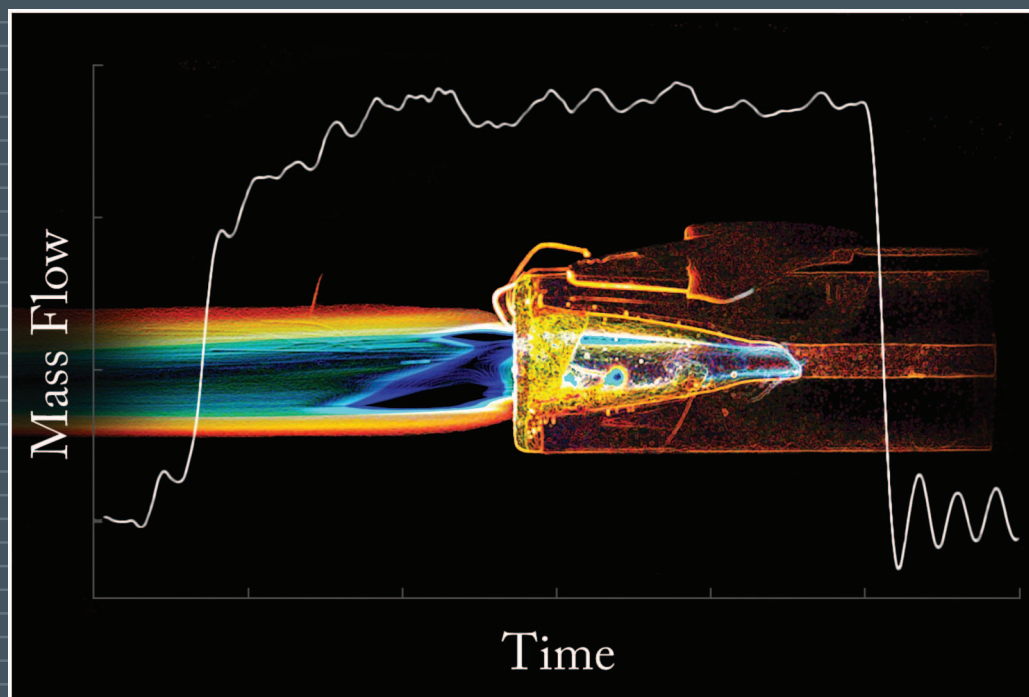


OCTOBER 2008

VOLUME 79 NUMBER 10

PART I

REVIEW OF SCIENTIFIC INSTRUMENTS



*INVITED ARTICLE: Time accurate mass flow measurements of solid-fueled systems
by Jordan D. Olliges, Taylor C. Lilly, Thomas B. Joslyn, and Andrew D. Ketsdever*



0034-6748(200810)79:10:1;1-4

AMERICAN
INSTITUTE
OF PHYSICS

- **Cover image** from Jordan D. Olliges, Taylor C. Lilly, Thomas B. Joslyn, and Andrew D. Ketsdever, *Rev. Sci. Instrum.* **79**, 101301 (2008). False color photograph of an acrylic (PMMA) hybrid motor fuel grain (black and blue correspond to regions of high spectral intensity). The region of high intensity inside the fuel grain is from the ignition system. Hybrid rocket firings were used to demonstrate time accurate mass flow measurements in solid-fueled systems.

INVITED ARTICLE

- 101301 **Invited Article: Time accurate mass flow measurements of solid-fueled systems** (7 pages)
Jordan D. Olliges, Taylor C. Lilly, Thomas B. Joslyn,
and Andrew D. Ketsdever
- OPTICS; ATOMS AND MOLECULES; SPECTROSCOPY; PHOTON DETECTORS
- 103101 **Development of high resolution Michelson interferometer for stable phase-locked ultrashort pulse pair generation** (7 pages)
Takumi Okada, Kazuhiro Komori, Keishiro Goshima,
Shohgo Yamauchi, Isao Morohashi, Takeyoshi Sugaya,
Mutsuo Ogura, and Noriaki Tsurumachi
- 103102 **A new magneto-optical trap-target recoil ion momentum spectroscopy apparatus for ion-atom collisions and trapped atom studies** (11 pages)
J. Blicck, X. Fléchar, A. Cassimi, H. Gilles, S. Girard,
and D. Hennecart
- 103103 **300 mm reference wafer fabrication by using direct laser lithography** (5 pages)
Hyug-Gyo Rhee, Dongik Kim, Seung-Ki Hong, and Yun-Woo Lee
- 103104 **A widely tunable laser frequency offset lock with digital counting** (7 pages)
Joshua Hughes and Chad Fertig
- 103105 **Portable light-emitting diode-based photometer with one-shot optochemical sensors for measurement in the field** (8 pages)
A. J. Palma, J. M. Ortigosa, A. Lapresta-Fernández,
M. D. Fernández-Ramos, M. A. Carvajal, and L. F. Capitán-Vallvey
- 103106 **Rapid photorefectance spectroscopy for strained silicon metrology** (3 pages)
H. Chouaib, M. E. Murtagh, V. Guènebaut, S. Ward, P. V. Kelly,
M. Kennard, Y. M. Le Vaillant, M. G. Somekh, M. C. Pitter,
and S. D. Sharples
- 103107 **Probing thermal waves on the free surface of various media: Surface fluctuation specular reflection spectroscopy** (7 pages)
A. Tay, C. Thibierge, D. Fournier, C. Fretigny, F. Lequeux,
C. Monteux, J. P. Roger, and L. Talini
- 103108 **Extreme-ultraviolet polarimeter utilizing laser-generated high-order harmonics** (7 pages)
Nicole Brimhall, Matthew Turner, Nicholas Herrick, David D. Allred,
R. Steven Turley, Michael Ware, and Justin Peatross

103109 **High-resolution imaging spectrometer for recording absolutely calibrated far ultraviolet spectra from laser-produced plasmas** (11 pages)
Charles M. Brown, John F. Seely, Uri Feldman, Glenn E. Holland,
James L. Weaver, Steven P. Obenschain,
Benjawan Kjornrattanawanich, and Drew Fielding

103110 **A frequency stabilization technique for diode lasers based on frequency-shifted beams from an acousto-optic modulator** (6 pages)
Mevan Gunawardena, Paul W. Hess, Jared Strait,
and P. K. Majumder

PARTICLE SOURCES, OPTICS AND ACCELERATION; PARTICLE DETECTORS

103301 **Generation and dose distribution measurement of flash x-ray in KALI-5000 system** (5 pages)
Rakhee Menon, Amitava Roy, S. Mitra, A. Sharma, J. Mondal,
K. C. Mittal, K. V. Nagesh, and D. P. Chakravarthy

103302 **The use and characterization of a backilluminated charge-coupled device in investigations of pulsed x-ray and radiation sources** (8 pages)
Wilfred Fullagar, Jens Uhlig, Monika Walczak, Sophie Canton,
and Villy Sundström

NUCLEAR PHYSICS, FUSION AND PLASMAS

103501 **Four free parameter empirical parametrization of glow discharge Langmuir probe data** (6 pages)
A. A. Azooz

103502 **Diagnosis of high-intensity pulsed heavy ion beam generated by a novel magnetically insulated diode with gas puff plasma gun** (5 pages)
H. Ito, H. Miyake, and K. Masugata

103503 **High precision (14 bit), high density (octal) analog to digital converter for spectroscopy applications** (7 pages)
E. T. Subramaniam, Mamta Jain, R. K. Bhowmik, and Michel Tripon

103504 **Low temperature plasma diagnostics with tunable synchrotron vacuum ultraviolet photoionization mass spectrometry** (5 pages)
Jing Wang, Yuyang Li, Zhenyu Tian, Taichang Zhang, Fei Qi,
and Xiaoping Tao

103505 **A correlation electron cyclotron emission diagnostic and the importance of multifield fluctuation measurements for testing nonlinear gyrokinetic turbulence simulations** (8 pages)
A. E. White, L. Schmitz, W. A. Peebles, T. A. Carter, T. L. Rhodes,
E. J. Doyle, P. A. Gourdain, J. C. Hillesheim, G. Wang,
C. Holland, G. R. Tynan, M. E. Austin, G. R. McKee, M. W. Shafer,
K. H. Burrell, J. Candy, J. C. DeBoo, R. Prater, G. M. Staebler,
R. E. Waltz, and M. A. Makowski

MICROSCOPY AND IMAGING

103701 **A flexible, highly stable electrochemical scanning probe microscope for nanoscale studies at the solid-liquid interface** (7 pages)
A. Z. Stieg, H. I. Rasool, and J. K. Gimzewski

103702 **Robust Ohmic contact junctions between metallic tips and multiwalled carbon nanotubes for scanned probe microscopy** (4 pages)
Suenne Kim, Jeehoon Kim, Morgann Berg, and Alex de Lozanne

(Continued)

- 103703 **Real-time atomic force microscopy using mechanical resonator type scanner** (3 pages)
Yongho Seo, C. S. Choi, S. H. Han, and Seung-Jin Han
- 103704 **High bandwidth control of precision motion instrumentation** (14 pages)
Douglas A. Bristow, Jingyan Dong, Andrew G. Alleyne, Placid Ferreira, and Srinivas Salapaka
- 103705 **Optical trapping and surgery of living yeast cells using a single laser** (5 pages)
Jun Ando, Godofredo Bautista, Nicholas Smith, Katsumasa Fujita, and Vincent Ricardo Daria
- 103706 **Cross-talk compensation in atomic force microscopy** (7 pages)
Cagdas D. Onal, Bilsay Sümer, and Metin Sitti
- 103707 **Fabrication of optical tips from photonic crystal fibers** (5 pages)
Christine A. Carlson and Jörg C. Woehl
- 103708 **High resolution hard x-ray microscope on a second generation synchrotron source** (5 pages)
Yangchao Tian, Wenjie Li, Jie Chen, Longhua Liu, Gang Liu, Andrei Tkachuk, Jinping Tian, Ying Xiong, Jeff Gelb, George Hsu, and Wenbing Yun
- 103709 **Improvements to a cryosystem to observe ice nucleating in a variable pressure scanning electron microscope** (7 pages)
D. Waller, D. J. Stokes, and A. M. Donald
- 103710 **Electrical impedance tomography with an optimized calculable square sensor** (7 pages)
Zhang Cao, Huaxiang Wang, and Lijun Xu

CONDENSED MATTER; MATERIALS

- 103901 **Integrated setup for the fabrication and measurement of magnetoresistive nanoconstrictions in ultrahigh vacuum** (6 pages)
Daniel Stickler, Robert Frömter, Wei Li, André Kobs, and Hans Peter Oepen
- 103902 **A new procedure for the quantitative analysis of extended x-ray absorption fine structure data in total reflection geometry** (6 pages)
F. Benzi, I. Davoli, M. Rovezzi, and F. d'Acapito
- 103903 **Magnetic detection of high-resolution electron spin resonance using a microcantilever in the millimeter-wave region up to 240 GHz** (5 pages)
E. Ohmichi, N. Mizuno, M. Kimata, and H. Ohta
- 103904 **Development of UHV dynamic nanostencil for surface patterning** (5 pages)
Haiming Guo, David Martrou, Tomaso Zambelli, Erik Dujardin, and Sébastien Gauthier
- 103905 **A method for measuring the nonlinear response in dielectric spectroscopy through third harmonics detection** (10 pages)
C. Thibierge, D. L'Hôte, F. Ladieu, and R. Tourbot
- 103906 **Picovoltmeter for probing vortex dynamics in a single weak-pinning Corbino channel** (4 pages)
T. W. Heitmann, K. Yu, C. Song, M. P. DeFeo, B. L. T. Plourde, M. B. S. Hesselberth, and P. H. Kes

(Continued)

- 103907 **Simple and precise thermoelectric power measurement setup for different environments** (5 pages)
L. S. Sharath Chandra, Archana Lakhani, Deepti Jain,
Swati Pandya, P. N. Vishwakarma, Mohan Gangrade,
and V. Ganesan
- 103908 **Surface force confinement cell for neutron reflectometry studies of complex fluids under nanoconfinement** (7 pages)
Jae-Hie J. Cho, Gregory S. Smith, William A. Hamilton,
Dennis J. Mulder, Tonya L. Kuhl, and Jimmy Mays

CHEMISTRY

- 104101 **Dopant-enhanced atmospheric pressure glow discharge ionization source for ion mobility spectrometry** (7 pages)
Can Dong, Lina Wang, Weiguo Wang, Keyou Hou, and Haiyang Li
- 104102 **Instrument and methods for surface dilatational rheology measurements** (10 pages)
Stoyan C. Russev, Nikola Alexandrov, Krastanka G. Marinova,
Krassimir D. Danov, Nikolai D. Denkov, Lyudmil Lyutov,
Vassil Vulchev, and Christine Bilke-Krause
- 104103 **The multiplexed chemical kinetic photoionization mass spectrometer: A new approach to isomer-resolved chemical kinetics** (10 pages)
David L. Osborn, Peng Zou, Howard Johnsen, Carl C. Hayden,
Craig A. Taatjes, Vadim D. Knyazev, Simon W. North,
Darcy S. Peterka, Musahid Ahmed, and Stephen R. Leone

BIOLOGY AND MEDICINE

- 104301 **A transistor based air flow transducer for thermohygrometric control of neonatal ventilatory applications** (7 pages)
Emiliano Schena and Sergio Silvestri
- 104302 **A system for high-speed microinjection of adherent cells** (6 pages)
Wenhui Wang, Yu Sun, Ming Zhang, Robin Anderson,
Lowell Langille, and Warren Chan

GRAVITY; GEOPHYSICS; ASTRONOMY AND ASTROPHYSICS

- 104501 **Feedback control of thermal lensing in a high optical power cavity** (5 pages)
Y. Fan, C. Zhao, J. Degallaix, L. Ju, D. G. Blair, B. J. J. Slagmolen,
D. J. Hosken, A. F. Brooks, P. J. Veitch, and J. Munch
- 104502 **A rocket-borne mass analyzer for charged aerosol particles in the mesosphere** (10 pages)
Scott Knappmiller, Scott Robertson, Zoltan Sternovsky,
and Martin Friedrich

ELECTRONICS; ELECTROMAGNETIC TECHNOLOGY; MICROWAVES

- 104701 **A method to measure the frequencies of individual half cells in a dumbbell cavity** (5 pages)
Sun An, Zhang Liping, Tang Yazhe, Ying-min Li, and Yong-Sub Cho
- 104702 **Sensitivity of the integrating pulse magnetometer with a first-order gradiometer** (8 pages)
S. Trojanowski and M. Ciszek

(Continued)

GENERAL INSTRUMENTS

- 105101 **A new mark shearing technique for strain measurement using digital image correlation method** (5 pages)
Tao Hua, Huimin Xie, Bing Pan, Qinghua Wang, and Fulong Dai
- 105102 **Quartz microbalance device for transfer into ultrahigh vacuum systems** (3 pages)
F. Stavale, H. Niehus, and C. A. Achete
- 105103 **Optical beam profile monitor and residual gas fluorescence at the relativistic heavy ion collider polarized hydrogen jet** (12 pages)
T. Tsang, S. Bellavia, R. Connolly, D. Gassner, Y. Makdisi, T. Russo, P. Thieberger, D. Trbojevic, and A. Zelenski
- 105104 **Development of a fast position-sensitive laser beam detector** (3 pages)
Isaac Chavez, Rongxin Huang, Kevin Henderson, Ernst-Ludwig Florin, and Mark G. Raizen
- 105105 **The simulator for icy world interiors: A 700 MPa pressure system for impulsive stimulated scattering and other optical measurements, with thermal control from -20 to 100 °C** (5 pages)
Steve Vance and J. Michael Brown

NOTES

- 106101 **10-fold detection range increase in quadrant-photodiode position sensing for photonic force microscope** (3 pages)
Sandro Perrone, Giovanni Volpe, and Dmitri Petrov
- 106102 **High speed scanning of terahertz pulse by a rotary optical delay line** (3 pages)
Geun-Ju Kim, Seok-Gy Jeon, Jung-Il Kim, and Yun-Sik Jin
- 106103 **Polarization-electric field hysteresis of ferroelectric PVDF films: Comparison of different measurement regimes** (3 pages)
Michael Wegener
- 106104 **Density measurement of shock compressed foam using two-dimensional x-ray radiography** (3 pages)
Sebastien Le Pape, Andrew Macphee, Daniel Hey, Pravesh Patel, Andrew Mackinnon, Mike Key, John Pasley, Mingsheng Wei, Sophia Chen, Tammy Ma, Farhat Beg, N. Alexander, Rich Stephens, Dustin Offerman, A. Link, Lynn Van-Woerkom, and R. Freeman
- 106105 **Fourier transform white-light interferometry based spatial frequency-division multiplexing of extrinsic Fabry-Pérot interferometric sensors** (3 pages)
Yi Jiang and Caijie Tang
- 106106 **A short-pulse K_a -band instrumentation radar for foliage attenuation measurements** (3 pages)
Mikko Puranen and Pekka Eskelinen
- 106107 **An infrared filter radiometer for atmospheric cluster-ion detection** (3 pages)
K. L. Aplin and R. A. McPheat
- A19 **NEW PRODUCTS** (4 pages)
- A23 **CUMULATIVE AUTHOR INDEX** (18 pages)

PROCEEDINGS OF THE 17TH TOPICAL CONFERENCE ON
HIGH-TEMPERATURE PLASMA DIAGNOSTICS

- 10E101 **Preface: Proceedings of the 17th Topical Conference on High-Temperature Plasma Diagnostics, Albuquerque, NM, 2008** (1 page)
Ramon J. Leeper
- X-RAY SPECTROSCOPY, X-RAY POWER, BOLOMETRY, AND OPACITY
MEASUREMENTS—*JAMES P. KNAUER, SESSION CHAIRMAN*
- 10E301 **Development of imaging bolometers for magnetic fusion reactors** (invited) (6 pages)
Byron J. Peterson, Homaira Parchamy, Naoko Ashikawa,
Hisato Kawashima, Shigeru Konoshima, Artem Yu. Kostyukov,
Igor V. Miroshnikov, Dongcheol Seo, and T. Omori
- 10E302 **Spatially resolved high resolution x-ray spectroscopy for magnetically confined fusion plasmas** (invited) (6 pages)
A. Ince-Cushman, J. E. Rice, M. Bitter, M. L. Reinke, K. W. Hill,
M. F. Gu, E. Eikenberry, Ch. Broennimann, S. Scott, Y. Podpaly,
S. G. Lee, and E. S. Marmor
- 10E303 **OZSPEC-2: An improved broadband high-resolution elliptical crystal x-ray spectrometer for high-energy density physics experiments** (invited) (6 pages)
R. F. Heeter, S. G. Anderson, R. Booth, G. V. Brown, J. Emig,
S. Fulkerson, T. McCarville, D. Norman, M. B. Schneider,
and B. K. F. Young
- 10E304 **Photoconductive detectors with fast temporal response for laser produced plasma experiments** (3 pages)
M. J. May, C. Halvorson, T. Perry, F. Weber, P. Young,
and C. Silbernagel
- 10E305 **A Bremsstrahlung spectrometer using *k*-edge and differential filters with image plate dosimeters** (3 pages)
C. D. Chen, J. A. King, M. H. Key, K. U. Akli, F. N. Beg, H. Chen,
R. R. Freeman, A. Link, A. J. Mackinnon, A. G. MacPhee,
P. K. Patel, M. Porkolab, R. B. Stephens, and L. D. Van Woerkom
- 10E306 **Time-resolved voltage measurements of Z-pinch radiation sources with a vacuum voltmeter** (3 pages)
D. P. Murphy, R. J. Allen, B. V. Weber, R. J. Commisso,
J. P. Apruzese, D. G. Phipps, and D. Mosher
- 10E307 **Performance of the EBIT calorimeter spectrometer** (4 pages)
Frederick Scott Porter, John Gygax, Richard L. Kelley,
Caroline A. Kilbourne, Jonathan M. King, Peter Beiersdorfer,
Gregory V. Brown, Daniel B. Thorn, and Steven M. Kahn

- 10E308 **Diagnostic of charge balance in high-temperature tungsten plasmas using LLNL EBIT** (3 pages)
G. C. Osborne, A. S. Safronova, V. L. Kantsyrev, U. I. Safronova, M. F. Yilmaz, K. M. Williamson, I. Shrestha, and P. Beiersdorfer
- 10E309 **Rapid, absolute calibration of x-ray filters employed by laser-produced plasma diagnostics** (3 pages)
G. V. Brown, P. Beiersdorfer, J. Emig, M. Frankel, M. F. Gu, R. F. Heeter, E. Magee, D. B. Thorn, K. Widmann, R. L. Kelley, C. A. Kilbourne, and F. S. Porter
- 10E310 **Analysis of time-resolved argon line spectra from OMEGA direct-drive implosions** (3 pages)
R. Florido, T. Nagayama, R. C. Mancini, R. Tommasini, J. A. Delettrez, S. P. Regan, V. A. Smalyuk, R. Rodríguez, and J. M. Gil
- 10E311 **High order reflectivity of highly oriented pyrolytic graphite crystals for x-ray energies up to 22 keV** (3 pages)
T. Döppner, P. Neumayer, F. Girard, N. L. Kugland, O. L. Landen, C. Niemann, and S. H. Glenzer
- 10E312 **Electron heated target temperature measurements in petawatt laser experiments based on extreme ultraviolet imaging and spectroscopy** (3 pages)
T. Ma, F. N. Beg, A. G. MacPhee, H.-K. Chung, M. H. Key, A. J. Mackinnon, P. K. Patel, S. Hatchett, K. U. Akli, R. B. Stephens, C. D. Chen, R. R. Freeman, A. Link, D. T. Offermann, V. Ovchinnikov, and L. D. Van Woerkom
- 10E313 **L-shell spectroscopy of Au as a temperature diagnostic tool** (3 pages)
E. Träbert, S. B. Hansen, P. Beiersdorfer, G. V. Brown, K. Widmann, and H.-K. Chung
- 10E314 **High resolution soft x-ray spectroscopy of low Z K-shell emission from laser-produced plasmas** (4 pages)
J. Dunn, E. W. Magee, R. Shepherd, H. Chen, S. B. Hansen, S. J. Moon, G. V. Brown, M.-F. Gu, P. Beiersdorfer, and M. A. Purvis
- 10E315 **X-ray diagnostics of imploding plasmas from planar wire arrays composed of Cu and few tracer Al wires on the 1MA pulsed power generator at UNR** (4 pages)
A. S. Safronova, V. L. Kantsyrev, A. A. Esaulov, N. D. Quart, M. F. Yilmaz, K. M. Williamson, V. Shlyaptseva, I. Shrestha, G. C. Osborne, C. A. Coverdale, B. Jones, and C. Deeney
- 10E316 **Measurements of high-current electron beams from X pinches and wire array Z pinches** (4 pages)
T. A. Shelkovenko, S. A. Pikuz, I. C. Blesener, R. D. McBride, K. S. Bell, D. A. Hammer, A. V. Agafonov, V. M. Romanova, and A. R. Mingaleev
- 10E317 **Spectral resolution measurement of an x-ray imaging crystal spectrometer for KSTAR** (3 pages)
S. G. Lee, J. G. Bak, U. W. Nam, M. K. Moon, J. K. Cheon, M. Bitter, and K. Hill
- 10E318 **Time-resolved x-ray and extreme ultraviolet spectrometer for use on the National Spherical Torus Experiment** (3 pages)
P. Beiersdorfer, J. K. Lepson, M. Bitter, K. W. Hill, and L. Roquemore

(Continued)

- 10E319 **Duplex multiwire proportional x-ray detector for multichord time-resolved soft x-ray and electron temperature measurements on T-10 tokamak** (3 pages)
A. V. Sushkov, V. F. Andreev, and D. E. Kravtsov
- 10E320 **A spatially resolving x-ray crystal spectrometer for measurement of ion-temperature and rotation-velocity profiles on the Alcator C-Mod tokamak** (4 pages)
K. W. Hill, M. L. Bitter, S. D. Scott, A. Ince-Cushman, M. Reinke, J. E. Rice, P. Beiersdorfer, M.-F. Gu, S. G. Lee, Ch. Broennimann, and E. F. Eikenberry
- 10E321 **An original calibration technique for soft x-ray detectors and its use in the Tore Supra tomographic system** (3 pages)
D. Mazon, D. Pacella, P. Malard, D. Garnier, A. Romano, and C. Bouchand
- 10E322 **Characterization of detection efficiency as function of energy for soft x-ray detectors** (3 pages)
D. Pacella, D. Mazon, A. Romano, P. Malard, and G. Pizzicaroli
- 10E323 **High-resolution hard x-ray spectroscopy of high-temperature plasmas using an array of quantum microcalorimeters** (3 pages)
Daniel B. Thorn, Ming F. Gu, Greg V. Brown, Peter Beiersdorfer, F. Scott Porter, Caroline A. Kilbourne, and Richard L. Kelley
- 10E324 **Method to estimate the electron temperature and neutral density in a plasma from spectroscopic measurements using argon atom and ion collisional-radiative models** (3 pages)
Ella M. Sciamma, Roger D. Bengtson, W. L. Rowan, Amy Keesee, Charles A. Lee, Dan Berisford, Kevin Lee, and K. W. Gentle
- FUSION PRODUCTS AND FAST IONS—JEFFREY A. KOCH,
SESSION CHAIRMAN
- 10E501 **Commissioning activities and first results from the collective Thomson scattering diagnostic on ASDEX Upgrade (invited)** (8 pages)
F. Meo, H. Bindslev, S. B. Korsholm, V. Furtula, F. Leuterer, F. Leipold, P. K. Michelsen, S. K. Nielsen, M. Salewski, J. Stober, D. Wagner, and P. Woskov
- 10E502 **First measurements of the absolute neutron spectrum using the magnetic recoil spectrometer at OMEGA (invited)** (6 pages)
J. A. Frenje, D. T. Casey, C. K. Li, J. R. Rygg, F. H. Séguin, R. D. Petrasso, V. Yu Glebov, D. D. Meyerhofer, T. C. Sangster, S. Hatchett, S. Haan, C. Cerjan, O. Landen, M. Moran, P. Song, D. C. Wilson, and R. J. Leeper
- 10E503 **Prompt radiochemistry at the National Ignition Facility (invited)** (5 pages)
G. P. Grim, P. A. Bradley, T. A. Bredeweg, A. L. Keksis, M. M. Fowler, A. C. Hayes, G. Jungman, A. W. Obst, R. S. Rundberg, D. J. Vieira, J. B. Wilhelmy, L. A. Bernstein, C. J. Cerjan, R. J. Fortner, K. J. Moody, D. H. Schneider, D. A. Shaughnessy, W. Stoeffl, and M. A. Stoyer
- 10E504 **In-vessel activation monitors in JET: Progress in modeling** (4 pages)
Georges Bonheure, I. Lengar, B. Syme, Elisabeth Wieslander, Mikael Hult, Joël Gasparro, Gerd Marissens, Dirk Arnold, Matthias Laubenstein, S. Popovichev, and JET-EFDA Contributors
- 10E505 **In-vessel design of ITER diagnostic neutron activation system** (3 pages)
M. S. Cheon, S. Pak, H. G. Lee, L. Bertalot, and C. Walker

(Continued)

- 10E506 **Absolute calibration of microfission chamber in JT-60U** (3 pages)
Takao Hayashi, Takeo Nishitani, Atsuhiko M. Sukegawa,
Masao Ishikawa, and Kouji Shinohara
- 10E507 **Design of microfission chamber for ITER operations** (4 pages)
Masao Ishikawa, Takashi Kondoh, Takeo Nishitani,
and Yoshinori Kusama
- 10E508 **Neutron spectrometer for ITER using silicon detectors** (3 pages)
Sean W. Conroy, Matthias Weiszflog, Erik Andersson-Sunden,
Goran Ericsson, Maria Gatu-Johnson, Carl Hellesen,
Emanuel Ronchi, and Henrik Sjostrand
- 10E509 **High repetition rate neutron flux array using digital-signal processing and scintillators for study of high performance plasma at JT-60U** (4 pages)
K. Shinohara, T. Okuji, M. Ishikawa, M. Baba, and T. Itoga
- 10E510 **Validating TRANSP simulations using neutron emission spectroscopy with dual sight lines** (4 pages)
C. Hellesen, E. A. Sundén, S. Conroy, G. Ericsson, L. Giacomelli,
A. Hjalmarsson, M. G. Johnsson, J. Källne, E. Ronchi,
M. Weiszflog, L. Ballabio, G. Gorini, M. Tardocchi, I. Voitsekhovitch,
and JET-EFDA Contributors
- 10E511 **Line integration effects on ion temperatures in tokamak plasmas measured with neutron emission spectroscopy** (4 pages)
F. Ognissanto, G. Gorini, M. Tardocchi, M. Albergante, L. Ballabio,
S. Conroy, and J. Källne
- 10E512 **Full orbit calculation for lost alpha particle measurement on ITER** (3 pages)
D. Funaki, M. Isobe, M. Nishiura, Y. Sato, A. Okamoto, T. Kobuchi,
S. Kitajima, and M. Sasao
- 10E513 **A neural networks framework for real-time unfolding of neutron spectroscopic data at JET** (4 pages)
E. Ronchi, S. Conroy, E. A. Sundén, G. Ericsson, A. Hjalmarsson,
C. Hellesen, M. G. Johnson, M. Weiszflog, and JET-EFDA
Contributors
- 10E514 **Neutron emission spectroscopy results for internal transport barrier and mode conversion ion cyclotron resonance heating experiments at JET** (4 pages)
L. Giacomelli, A. Hjalmarsson, J. Källne, C. Hellesen, M. Tardocchi,
G. Gorini, D. Van Eester, E. Lerche, T. Johnson, V. Kiptily,
S. Conroy, E. Andersson Sundén, G. Ericsson, M. Gatu Johnson,
H. Sjöstrand, M. Weiszflog, and JET-EFDA Contributors
- 10E515 **Application of a digital pileup resolving method to high count rate neutron measurements** (3 pages)
Francesco Belli, Basilio Esposito, Daniele Marocco, Marco Riva,
and Andreas Zimbal
- 10E516 **The response of a radiation resistant ceramic scintillator ($\text{Al}_2\text{O}_3:\text{Cr}$) to low energy ions (0–60 keV)** (3 pages)
D. Jimenez-Rey, B. Zurro, K. J. McCarthy, G. Garcia,
and A. Baciero
- 10E517 **Investigating the possibility of a monitoring fast ion diagnostic for ITER** (3 pages)
R. De Angelis, M. G. von Hellermann, F. P. Orsitto, and S. Tugarinov

(Continued)

- 10E518 **Pellet charge exchange helium measurement using neutral particle analyzer in large helical device** (4 pages)
T. Ozaki, P. Goncharov, E. Veshchev, N. Tamura, S. Sudo,
T. Seki, H. Kasahara, Y. Takase, and T. Ohsako
- 10E519 **Fast ion charge exchange spectroscopy measurement using a radially injected neutral beam on the large helical device** (4 pages)
Masaki Osakabe, Sadayoshi Murakami, Mikiro Yoshinuma,
Katsumi Ida, Allan Whiteford, Motoshi Goto, Daiji Kato,
Takako Kato, Kenichi Nagaoka, Tokihiko Tokuzawa,
Yasuhiko Takeiri, and Osamu Kaneko
- 10E520 **A new fast-ion D_α diagnostic for DIII-D** (4 pages)
W. W. Heidbrink, Y. Luo, C. M. Muscatello, Y. Zhu, and K. H. Burrell
- 10E521 **The NSTX fast-ion D-alpha diagnostic** (5 pages)
M. Podestà, W. W. Heidbrink, R. E. Bell, and R. Feder
- 10E522 **Charge exchange spectroscopy as a fast ion diagnostic on TEXTOR** (4 pages)
E. Delabie, R. J. E. Jaspers, M. G. von Hellermann, S. K. Nielsen,
and O. Marchuk
- 10E523 **Fast ion measurement using a hybrid directional probe in the large helical device** (3 pages)
Kenichi Nagaoka, Kiyomasa Y. Watanabe, Masaki Osakabe,
Yasuhiko Takeiri, Takashi Minami, Kazuo Toi, Mitsutaka Isobe,
Masaki Nishiura, Takafumi Ito, and Kunihiro Ogawa
- 10E524 **Gamma ray spectroscopy at high energy and high time resolution at JET** (4 pages)
M. Tardocchi, L. I. Proverbio, G. Gorini, G. Grosso, M. Locatelli,
I. N. Chugonov, D. B. Gin, A. E. Shevelev, A. Murari, V. G. Kiptily,
B. Syme, A. M. Fernandes, R. C. Pereira, J. Sousa,
and JET-EFDA Contributors
- 10E525 **Diagnosing ignition with DT reaction history** (4 pages)
D. C. Wilson, P. A. Bradley, C. J. Cerjan, J. D. Salmonson,
B. K. Spears, S. P. Hatchet, II, H. W. Herrmann, and V. Yu. Glebov
- 10E526 **Use of $d\text{-}^3\text{He}$ proton spectroscopy as a diagnostic of shell ρr in capsule implosion experiments with ~ 0.2 NIF scale high temperature Hohlraums at Omega** (4 pages)
N. D. Delamater, D. C. Wilson, G. A. Kyrala, A. Seifter,
N. M. Hoffman, E. Dodd, R. Singleton, V. Glebov, C. Stoeckl,
C. K. Li, R. Petrasso, and J. Frenje
- 10E527 **Tests and calibration of NIF neutron time of flight detectors** (4 pages)
Z. A. Ali, V. Yu. Glebov, M. Cruz, T. Duffy, C. Stoeckl, S. Roberts,
T. C. Sangster, R. Tommasini, A. Throop, M. Moran, L. Dauffy,
and C. Horsefield
- 10E528 **Neutron bang time detector based on a light pipe** (3 pages)
V. Yu. Glebov, M. Moran, C. Stoeckl, T. C. Sangster, and M. Cruz

(Continued)

- 10E529 **The National Ignition Facility Neutron Imaging System** (5 pages)
 Mark D. Wilke, Steven H. Batha, Paul A. Bradley, Robert D. Day,
 David D. Clark, Valerie E. Fatherley, Joshua P. Finch,
 Robert A. Gallegos, Felix P. Garcia, Gary P. Grim,
 Steven A. Jaramillo, Andrew J. Montoya, Michael J. Moran,
 George L. Morgan, John A. Oertel, Thomas A. Ortiz,
 Jeremy R. Payton, Peter Pazuchanics, Derek W. Schmidt,
 Adelaida C. Valdez, Carl H. Wilde, and Doug C. Wilson
- 10E530 **One-dimensional neutron imager for the Sandia Z facility** (4 pages)
 David N. Fittinghoff, Dan E. Bower, James R. Hollaway,
 Barry A. Jacoby, Paul B. Weiss, Robert A. Buckles,
 Timothy J. Sammons, Leroy A. McPherson, Jr., Carlos L. Ruiz,
 Gordon A. Chandler, José A. Torres, Ramon J. Leeper,
 Gary W. Cooper, and Alan J. Nelson
- 10E531 **Cherenkov radiation conversion and collection considerations for a gamma bang time/reaction history diagnostic for the NIF** (3 pages)
 Hans W. Herrmann, Joseph M. Mack, Carlton S. Young,
 Robert M. Malone, Wolfgang Stoeffl, and Colin J. Horsfield
- 10E532 **Gamma bang time/reaction history diagnostics for the National Ignition Facility using 90° off-axis parabolic mirrors** (2 pages)
 R. M. Malone, H. W. Herrmann, W. Stoeffl, J. M. Mack,
 and C. S. Young
- 10E533 **High performance compact magnetic spectrometers for energetic ion and electron measurement in ultraintense short pulse laser solid interactions** (3 pages)
 Hui Chen, Anthony J. Link, Roger van Maren, Pravesh K. Patel,
 Ronnie Shepherd, Scott C. Wilks, and Peter Beiersdorfer
- 10E534 **Scaling laws for energetic ions from the commissioning of the new Los Alamos National Laboratory 200 TW Trident laser** (4 pages)
 K. A. Flippo, J. Workman, D. C. Gautier, S. Letzring, R. P. Johnson,
 and T. Shimada
- 10E535 **Characterization of radiochromic film scanning techniques used in short-pulse-laser ion acceleration** (5 pages)
 Joseph S. Cowan, Kirk A. Flippo, and Sandrine A. Gaillard
- 10E536 **A simple apparatus for quick qualitative analysis of CR39 nuclear track detectors** (3 pages)
 D. C. Gautier, J. L. Kline, K. A. Flippo, S. A. Gaillard, S. A. Letzring,
 and B. M. Hegelich
- 10E537 **A spatially resolved ion temperature diagnostic for the National Ignition Facility** (3 pages)
 G. P. Grim, J. P. Finch, N. S. P. King, G. L. Morgan, J. A. Oertel,
 C. H. Wilde, M. D. Wilke, D. C. Wilson, and D. E. Johnson
- INTERFEROMETRY, POLARIMETRY, THOMSON SCATTERING,
 BACKSCATTERING, AND FLUCTUATIONS—DAVID L. BROWER,
 SESSION CHAIRMAN
- 10E701 **Measurement of magnetic fluctuation-induced particle flux (invited)** (5 pages)
 W. X. Ding, D. L. Brower, and T. Y. Yates

(Continued)

- 10E702 **Two-dimensional phase contrast imaging for local turbulence measurements in large helical device (invited)** (7 pages)
K. Tanaka, C. A. Michael, L. N. Vyacheslavov, A. L. Sanin,
K. Kawahata, T. Akiyama, T. Tokuzawa, and S. Okajima
- 10E703 **Nonperturbative measurement of the *local* magnetic field using pulsed polarimetry for fusion reactor conditions (invited)** (8 pages)
Roger J. Smith
- 10E704 **Imaging interferometers for analysis of Thomson scattered spectra** (3 pages)
J. Howard and T. Hatae
- 10E705 **A 280 GHz single-channel millimeter-wave interferometer system for KSTAR** (3 pages)
Y. U. Nam and K. D. Lee
- 10E706 **Radial density profile measurement by using the multichannel microwave interferometer in GAMMA 10** (3 pages)
M. Yoshikawa, T. Matsumoto, Y. Shima, S. Negishi, Y. Miyata,
M. Mizuguchi, N. Imai, Y. Yoneda, H. Hojo, A. Itakura, and T. Imai
- 10E707 **Development of terahertz laser diagnostics for electron density measurements** (4 pages)
K. Kawahata, T. Akiyama, K. Tanaka, K. Nakayama, and S. Okajima
- 10E708 **Development of a multichannel dispersion interferometer at TEXTOR** (3 pages)
A. Lizunov, P. Bagryansky, A. Khilchenko, Yu. V. Kovalenko,
A. Solomakhin, W. Biel, H. T. Lambertz, Yu. Krasikov, M. Mitri,
B. Schweer, and H. Dreier
- 10E709 **Dichroic filters to protect milliwatt far-infrared detectors from megawatt ECRH radiation** (4 pages)
G. Bertschinger, C. P. Endres, F. Lewen, and J. W. Oosterbeek
- 10E710 **Fringe jump analysis and electronic corrections for the Tore Supra far infrared interferometer** (4 pages)
C. Gil, A. Barbuti, D. Elbèze, P. Pastor, J. Philip, and L. Toulouse
- 10E711 **Real-time digital heterodyne interferometer for high resolution plasma density measurements at ISTTOK** (3 pages)
T. G. Marques, A. Gouveia, T. Pereira, J. Fortunato, B. B. Carvalho,
J. Sousa, C. Silva, and H. Fernandes
- 10E712 **Bayesian experimental design of a multichannel interferometer for Wendelstein 7-X** (3 pages)
H. Dreier, A. Dinklage, R. Fischer, M. Hirsch, and P. Kornejew
- 10E713 **Calibration of a high spatial resolution laser two-color heterodyne interferometer for density profile measurements in the TJ-II stellarator** (5 pages)
Pablo Acedo, P. Pedreira, A. R. Criado, Horacio Lamela,
Miguel Sánchez, and Joaquín Sánchez
- 10E714 **Simultaneous density and magnetic field fluctuation measurements by far-infrared interferometry and polarimetry in MST** (3 pages)
T. F. Yates, W. X. Ding, T. A. Carter, and D. L. Brower
- 10E715 **Spectroscopic interferometer for coherence length spectroscopy of pulsed discharge plasma** (4 pages)
Yong W. Kim and Nopporn Poolyarat

(Continued)

- 10E716 **A torquing shearing interferometer for cylindrical wire array experiments** (3 pages)
S. A. Pikuz, P. C. Schrafel, T. A. Shelkovenko, and B. R. Kusse
- 10E717 **A comparison of planar, laser-induced fluorescence, and high-sensitivity interferometry techniques for gas-puff nozzle density measurements** (4 pages)
S. L. Jackson, B. V. Weber, D. Mosher, D. G. Phipps,
S. J. Stephanakis, R. J. Comisso, N. Qi, B. H. Failor,
and P. L. Coleman
- 10E718 **Real-time electron density measurements from Cotton–Mouton effect in JET machine** (3 pages)
M. Brombin, A. Boboc, L. Zabeo, A. Murari, and JET-EFDA
Contributors
- 10E719 **CO₂ laser polarimeter for Faraday rotation measurements in the DIII-D tokamak** (3 pages)
M. A. Van Zeeland, R. L. Boivin, T. N. Carlstrom, and T. M. Deterly
- 10E720 **Short wavelength far infrared laser polarimeter with silicon photoelastic modulators** (5 pages)
T. Akiyama, K. Kawahata, K. Tanaka, S. Okajima, and K. Nakayama
- 10E721 **Collective backscattering of gyrotron radiation by small-scale plasma density fluctuations in large helical device** (4 pages)
Nikolay Kharchev, Kenji Tanaka, Shin Kubo, Hiroe Igami,
German Batanov, Alexandr Petrov, Karen Sarksyian,
Nina Skvortsova, Yoshifumi Azuma, and Shunji Tsuji-lio
- 10E722 **The observation of nonlinear ion cyclotron wave excitation during high-harmonic fast wave heating in the large helical device** (4 pages)
H. Kasahara, T. Seki, R. Kumazawa, K. Saito, T. Mutoh, S. Kubo,
T. Shimozuma, H. Igami, Y. Yoshimura, H. Takahashi, I. Yamada,
T. Tokuzawa, S. Ohdachi, S. Morita, G. Nomura, F. Shimpō,
A. Komori, O. Motojima, T. Oosako, Y. Takase, Y. Zhao, and J. Kwak
- 10E723 **Spatial resolution study and power calibration of the high-*k* scattering system on NSTX** (3 pages)
W. Lee, H. K. Park, M. H. Cho, W. Namkung, D. R. Smith,
C. W. Domier, and N. C. Luhmann, Jr.
- 10E724 **Detection of high *k* turbulence using two dimensional phase contrast imaging on LHD** (5 pages)
C. A. Michael, K. Tanaka, L. N. Vyacheslavov, A. Sanin,
N. K. Kharchev, T. Akiyama, K. Kawahata, and S. Okajima
- 10E725 **A 300 GHz collective scattering diagnostic for low temperature plasmas** (3 pages)
Robert A. Hardin, Earl E. Scime, and John Heard
- 10E726 **Design study of polychromators for ITER edge Thomson scattering diagnostics** (4 pages)
Shin Kajita, Takaki Hatae, and Yoshinori Kusama
- 10E727 **ITER LIDAR performance analysis** (5 pages)
M. N. A. Beurskens, L. Giudicotti, M. Kempenaars, R. Scannell,
and M. J. Walsh
- 10E728 **Enhancement of the JET edge LIDAR Thomson scattering diagnostic with ultrafast detectors** (4 pages)
M. Kempenaars, J. C. Flanagan, L. Giudicotti, M. J. Walsh,
M. Beurskens, I. Balboa, and JET-EFDA Contributors

(Continued)

- 10E729 **Investigation of first mirror heating for the collective Thomson scattering diagnostic in ITER** (5 pages)
M. Salewski, F. Meo, H. Bindslev, V. Furtula, S. B. Korsholm, B. Lauritzen, F. Leipold, P. K. Michelsen, S. K. Nielsen, and E. Nonbøl
- 10E730 **Design of a new Nd:YAG Thomson scattering system for MAST** (4 pages)
R. Scannell, M. J. Walsh, P. G. Carolan, A. C. Darke, M. R. Dunstan, R. B. Huxford, G. McArdle, D. Morgan, G. Naylor, T. O'Gorman, S. Shibaev, N. Barratt, K. J. Gibson, G. J. Tallents, and H. R. Wilson
- 10E731 **Design of collective Thomson scattering system using 77 GHz gyrotron for bulk and tail ion diagnostics in the large helical device** (3 pages)
M. Nishiura, K. Tanaka, S. Kubo, T. Saito, Y. Tatematsu, T. Notake, K. Kawahata, T. Shimozuma, and T. Mutoh
- 10E732 **Subterahertz gyrotron developments for collective Thomson scattering in LHD** (3 pages)
T. Notake, T. Saito, Y. Tatematsu, S. Kubo, T. Shimozuma, K. Tanaka, M. Nishiura, A. Fujii, La Agusu, I. Ogawa, and T. Idehara
- 10E733 **Multipoint Thomson scattering diagnostic for the Madison Symmetric Torus reversed-field pinch** (5 pages)
J. A. Reusch, M. T. Borchardt, D. J. Den Hartog, A. F. Falkowski, D. J. Holly, R. O'Connell, and H. D. Stephens
- 10E734 **Calibration of a Thomson scattering diagnostic for fluctuation measurements** (5 pages)
H. D. Stephens, M. T. Borchardt, D. J. Den Hartog, A. F. Falkowski, D. J. Holly, R. O'Connell, and J. A. Reusch
- 10E735 **Optimizing a Thomson scattering diagnostic for fast dynamics and high background** (5 pages)
R. O'Connell, D. J. Den Hartog, M. T. Borchardt, D. J. Holly, J. A. Reusch, and H. D. Stephens
- 10E736 **A pulse-burst laser system for a high-repetition-rate Thomson scattering diagnostic** (4 pages)
D. J. Den Hartog, N. Jiang, and W. R. Lempert
- 10E737 **Thomson scattering density calibration by Rayleigh and rotational Raman scattering on NSTX** (4 pages)
B. P. LeBlanc
- 10E738 **The Thomson scattering system on the lithium tokamak experiment** (5 pages)
T. Strickler, R. Majeski, R. Kaita, and B. LeBlanc
- 10E739 **Demonstration of x-ray Thomson scattering using picosecond $K\text{-}\alpha$ x-ray sources in the characterization of dense heated matter** (3 pages)
A. L. Kritcher, P. Neumayer, H. J. Lee, T. Döppner, R. W. Falcone, S. H. Glenzer, and E. C. Morse

X-RAY IMAGING, X-RAY DETECTORS, AND RADIOGRAPHY—ROBERT L.
KAUFFMAN, SESSION CHAIRMAN

- 10E901 **Development of backlighting sources for a Compton radiography diagnostic of inertial confinement fusion targets (invited) (4 pages)**
R. Tommasini, A. MacPhee, D. Hey, T. Ma, C. Chen, N. Izumi, W. Unites, A. MacKinnon, S. P. Hatchett, B. A. Remington, H. S. Park, P. Springer, J. A. Koch, O. L. Landen, John Seely, Glenn Holland, and Larry Hudson
- 10E902 **Measurement and modeling of pulsed microchannel plate operation (invited) (6 pages)**
G. A. Rochau, M. Wu, C. Kruschwitz, N. Joseph, K. Moy, J. Bailey, M. Krane, R. Thomas, D. Nielsen, and A. Tibbitts
- 10E903 **NIF-scale re-emission sphere measurements of early-time $T_r=100$ eV hohlraum symmetry (invited) (6 pages)**
E. L. Dewald, C. Thomas, J. Milovich, J. Edwards, C. Sorce, R. Kirkwood, D. Meeker, O. Jones, N. Izumi, and O. L. Landen
- 10E904 **A versatile high-resolution x-ray imager (HRXI) for laser-plasma experiments on OMEGA (5 pages)**
J. L. Bourgade, P. Troussel, A. Casner, G. Huser, T. C. Sangster, G. Pien, F. J. Marshall, J. Fariaud, C. Remond, D. Gontier, C. Chollet, C. Zuber, C. Reverdin, A. Richard, P. A. Jaanimagi, R. L. Keck, R. E. Bahr, W. J. Armstrong, J. Dewandel, R. Maroni, F. Aubard, B. Angelier, C. Y. Cote, and S. Magnan
- 10E905 **High-energy, high-resolution x-ray imaging on the Trident short-pulse laser facility (3 pages)**
J. Workman, J. Cobble, K. Flippo, D. C. Gautier, and S. Letzring
- 10E906 **Multicolor, time-gated, soft x-ray pinhole imaging of wire array and gas puff Z pinches on the Z and Saturn pulsed power generators (4 pages)**
B. Jones, C. A. Coverdale, D. S. Nielsen, M. C. Jones, C. Deeney, J. D. Serrano, L. B. Nielsen-Weber, C. J. Meyer, J. P. Apruzese, R. W. Clark, and P. L. Coleman
- 10E907 **One-dimensional and multichannels multi-imaging x-ray streak camera for imploded core plasma of shell-cone target (4 pages)**
Jiayong Zhong, Hiroyuki Shiraga, and Hiroshi Azechi
- 10E908 **Monochromatic x-ray sampling streak imager for fast-ignitor plasma observation (3 pages)**
Minoru Tanabe, Takashi Fujiwara, Shinsuke Fujioka, Hiroaki Nishimura, Hiroyuki Shiraga, Hiroshi Azechi, and Kunioki Mima
- 10E909 **Measurement of heating laser injection time to imploded core plasma by using x-ray framing camera (3 pages)**
Mayuko Koga, Takashi Fujiwara, Tatsuhiro Sakaiya, Myongdok Lee, Keisuke Shigemori, Hiroyuki Shiraga, and Hiroshi Azechi
- 10E910 **Use of imaging plates at near saturation for high energy density particles (3 pages)**
Tsuyoshi Tanimoto, Kazuhide Ohta, Hideaki Habara, Toshinori Yabuuchi, Ryousuke Kodama, Motonobu Tampo, Jian Zheng, and Kazuo A. Tanaka

(Continued)

- 10E911 **Monte Carlo simulations of high-speed, time-gated microchannel-plate-based x-ray detectors: Saturation effects in dc and pulsed modes and detector dynamic range** (4 pages)
Craig A. Kruschwitz, Ming Wu, Ken Moy, and Greg Rochau
- 10E912 **Performance of Au transmission photocathode on a microchannel plate detector** (5 pages)
M. E. Lowenstern, E. C. Harding, C. M. Huntington, A. J. Visco, G. Rathore, and R. P. Drake
- 10E913 **Design of a streaked radiography instrument for ICF ablator tuning measurements** (3 pages)
R. E. Olson, D. G. Hicks, B. K. Spears, P. M. Celliers, J. P. Holder, O. L. Landen, M. Geissel, J. W. Kellogg, G. R. Bennett, A. D. Edens, B. W. Atherton, and R. J. Leeper
- 10E914 **2–20 ns interframe time 2-frame 6.151 keV x-ray imaging on the recently upgraded Z Accelerator: A progress report** (3 pages)
G. R. Bennett, I. C. Smith, J. E. Shores, D. B. Sinars, G. Robertson, B. W. Atherton, M. C. Jones, and J. L. Porter
- 10E915 **Long duration backlighter experiments at Omega** (3 pages)
A. B. Reighard, S. G. Glendinning, P. E. Young, W. W. Hsing, M. Foord, M. Schneider, K. Lu, T. Dittrich, R. Wallace, and C. Sorce
- 10E916 **Streaked x-ray backlighting with twin-slit imager for study of density profile and trajectory of low-density foam target filled with deuterium liquid** (3 pages)
H. Shiraga, N. Mahigashi, T. Yamada, S. Fujioka, T. Sakaiya, K. Shigemori, M. Nakai, H. Azechi, and A. Sunahara
- 10E917 **High contrast Kr gas jet $K\alpha$ x-ray source for high energy density physics experiments** (3 pages)
N. L. Kugland, P. Neumayer, T. Döppner, H.-K. Chung, C. G. Constantin, F. Girard, S. H. Glenzer, A. Kemp, and C. Niemann
- 10E918 **Conversion efficiency of high-Z backlighter materials** (3 pages)
Paul A. Keiter, Andrew Comely, John Morton, Heidi Tierney, Jonathan Workman, and Mark Taylor
- 10E919 **Blast wave energy diagnostic** (4 pages)
Thomas E. Tierney, IV, Heidi E. Tierney, George C. Idzorek, Robert G. Watt, Robert R. Peterson, Darrell L. Peterson, Christopher L. Fryer, Mike R. Lopez, Michael C. Jones, Daniel Sinars, Gregory A. Rochau, and James E. Bailey
- 10E920 **Observation of asymmetrically imploded core plasmas with a two-dimensional sampling image x-ray streak camera** (3 pages)
Hiroyuki Shiraga, Myongdok Lee, Norimitsu Mahigashi, Shinsuke Fujioka, and Hiroshi Azechi
- 10E921 **Comparison of genetic-algorithm and emissivity-ratio analyses of image data from OMEGA implosion cores** (4 pages)
T. Nagayama, R. C. Mancini, R. Florido, R. Tommasini, J. A. Koch, J. A. Delettrez, S. P. Regan, V. A. Smalyuk, L. A. Welser-Sherrill, and I. E. Golovkin
- 10E922 **Reproducible, rugged, and inexpensive photocathode x-ray diode** (3 pages)
G. C. Idzorek, T. E. Tierney, T. E. Lockard, K. J. Moy, and J. W. Keister

(Continued)

- 10E923 **Soft x-ray measurements using photoconductive type-IIa and single-crystal chemical vapor deposited diamond detectors** (3 pages)
A. S. Moore, C. D. Bentley, J. M. Foster, G. Goedhart, P. Graham, M. J. Taylor, and E. Hellewell
- 10E924 **Calibration and characterization of single photon counting cameras for short-pulse laser experiments** (4 pages)
B. R. Maddox, H. S. Park, B. A. Remington, and M. McKernan
- 10E925 **Flat field anomalies in an x-ray charge coupled device camera measured using a Manson x-ray source** (5 pages)
M. J. Haugh and M. B. Schneider
- 10E926 **Design and initial operation of multichord soft x-ray detection arrays on the STOR-M tokamak** (3 pages)
C. Xiao, T. Niu, J. E. Morelli, C. Paz-Soldan, M. Dreval, S. Elgriw, A. Pant, D. Rohraff, D. Trembach, and A. Hirose
- 10E927 **Wide-angle point-to-point x-ray imaging with almost arbitrarily large angles of incidence** (3 pages)
M. Bitter, K. W. Hill, S. Scott, R. Feder, Jinseok Ko, A. Ince-Cushman, and J. E. Rice
- 10E928 **Fast soft x-ray images of magnetohydrodynamic phenomena in NSTX** (4 pages)
C. E. Bush, B. C. Stratton, J. Robinson, L. E. Zakharov, E. D. Fredrickson, D. Stutman, and K. Tritz
- 10E929 **Energy resolved soft x-ray imaging using a charge coupled device camera for long pulse discharges in the Large Helical Device** (4 pages)
C. Suzuki, K. Ida, T. Kobuchi, and M. Yoshinuma
- 10E930 **The radiation-tolerant x-ray monitor** (3 pages)
Yu. V. Gott and M. M. Stepanenko
- 10E931 **Using x-rays to test chemical vapor deposited diamond detectors for areal density measurement at the National Ignition Facility** (3 pages)
L. S. Dauffy, J. A. Koch, R. Tommasini, and N. Izumi
- 10E932 **X-ray diagnostic calibration with the tabletop laser facility EQUINOX** (4 pages)
Charles Reverdin, M. Paurisse, T. Caillaud, P. Combis, A. Duval, D. Gontier, D. Husson, C. Rubbelynck, and C. Zuber
- REFLECTOMETRY, ECE, RF, MAGNETICS, AND PROBES—*TONY DONNÉ*,
SESSION CHAIRMAN
- 10F101 **Electron Bernstein wave emission based diagnostic on National Spherical Torus Experiment (invited)** (6 pages)
S. J. Diem, G. Taylor, J. B. Caughman, P. Efthimion, H. Kugel, B. P. LeBlanc, J. Preinhaelter, S. A. Sabbagh, J. Urban, and J. Wilgen
- 10F102 **Application of reflectometry power flow for magnetic field pitch angle measurements in tokamak plasmas (invited)** (8 pages)
P.-A. Gourdain and W. A. Peebles
- 10F103 **The next generation of electron cyclotron emission imaging diagnostics (invited)** (5 pages)
P. Zhang, C. W. Domier, T. Liang, X. Kong, B. Tobias, Z. Shen, N. C. Luhmann, Jr., H. Park, I. G. J. Classen, M. J. van de Pol, A. J. H. Donné, and R. Jaspers

(Continued)

- 10F104 **Study of ITER plasma position reflectometer using a two-dimensional full-wave finite-difference time domain code** (4 pages)
F. da Silva and S. Heurax
- 10F105 **Robust measurement of group delay in the presence of density fluctuations by means of ultrafast swept reflectometry** (4 pages)
Roberto Cavazzana and Maurizio Moresco
- 10F106 **High resolution fast wave reflectometry: JET design and implications for ITER** (4 pages)
L. Cupido, A. Cardinali, R. Igreja, F. Serra, M. E. Manso, A. Murari, and JET-EFDA Contributors
- 10F107 **Systematic and routine analysis of radial correlation reflectometry data in JET** (3 pages)
António C. A. Figueiredo, António Fonseca, Luís Meneses, and JET-EFDA Contributors
- 10F108 **First density profile measurements using frequency modulation of the continuous wave reflectometry on JET** (4 pages)
L. Meneses, L. Cupido, A. Sirinelli, M. E. Manso, and JET-EFDA Contributors
- 10F109 **V-band frequency hopping microwave reflectometer in LHD** (4 pages)
T. Tokuzawa, A. Ejiri, K. Kawahata, K. Tanaka, and Y. Ito
- 10F110 **Proposal of *in situ* density calibration for Thomson scattering measurement by microwave reflectometry** (4 pages)
Takashi Minami, Hisamichi Funaba, Kazumichi Narihara, Ichihiro Yamada, Hiroshi Hayashi, and Toshikazu Kohmoto
- 10F111 **Development of microwave imaging reflectometry in large helical device** (4 pages)
S. Yamaguchi, Y. Nagayama, D. Kuwahara, T. Yoshinaga, Z. B. Shi, Y. Kogi, and A. Mase
- 10F112 **Reconstruction of edge density profiles on Large Helical Device using ultrashort-pulse reflectometry** (3 pages)
Yuya Yokota, Atsushi Mase, Yuichiro Kogi, Tokihiko Tokuzawa, Kazuo Kawahata, Yoshio Nagayama, and Hitoshi Hojo
- 10F113 **Detection of zonal flow spectra in DIII-D by a dual-channel Doppler backscattering system** (3 pages)
L. Schmitz, G. Wang, J. C. Hillesheim, T. L. Rhodes, W. A. Peebles, A. E. White, L. Zeng, T. A. Carter, and W. Solomon
- 10F114 **Scrape-off layer reflectometer for Alcator C-Mod** (4 pages)
G. R. Hanson, J. B. Wilgen, C. Lau, Y. Lin, G. M. Wallace, and S. J. Wukitch
- 10F115 **Development of multichannel intermediate frequency system for electron cyclotron emission radiometer on KSTAR Tokamak** (3 pages)
Yuichiro Kogi, Takuya Sakoda, Atsushi Mase, Naoki Ito, Yuya Yokota, Soichiro Yamaguchi, Yoshio Nagayama, Seung H. Jeong, Myeun Kwon, and Kazuo Kawahata
- 10F116 **Magnetic diagnostics for the lithium tokamak experiment** (3 pages)
L. Berzak, R. Kaita, T. Kozub, R. Majeski, and L. Zakharov
- 10F117 **Magnetic diagnostics for the first plasma operation in Korea Superconducting Tokamak Advanced Research** (3 pages)
S. G. Lee, J. G. Bak, E. M. Ka, J. H. Kim, and S. H. Hahn

(Continued)

- 10F118 **Diamagnetic loop for the first plasma in the KSTAR machine** (4 pages)
J. G. Bak, S. G. Lee, and E. M. Ka
- 10F119 **Performance test of the integrator system for magnetic diagnostics in KSTAR** (3 pages)
E. M. Ka, S. G. Lee, J. G. Bak, and D. Son
- 10F120 **Poloidal mode analysis of magnetic probe data in a spherical tokamak configuration** (3 pages)
H. Tojo, A. Ejiri, M. P. Gryaznevich, Y. Takase, and Y. Adachi
- 10F121 **Real-time estimation of the poloidal wavenumber of ISTTOK tokamak magnetic fluctuations** (4 pages)
R. Coelho and D. Alves
- 10F122 **W7-X magnetic diagnostics: Rogowski coil performance for very long pulses** (4 pages)
Andreas Werner, Michael Endler, Joachim Geiger, and Ralf Koenig
- 10F123 **Magnetic measurements using array of integrated Hall sensors on the CASTOR tokamak** (3 pages)
Ivan Ďuran, Olena Hronová, Jan Stöckel, Jana Sentkerestiová, and Josef Havlicek
- 10F124 **Diagnostics for the biased electrode experiment on NSTX** (4 pages)
A. L. Roquemore, S. J. Zweben, R. Kaita, R. J. Marsalsa, C. E. Bush, and R. J. Maqueda
- 10F125 **High heat flux Langmuir probe array for the DIII-D divertor plates** (4 pages)
J. G. Watkins, D. Taussig, R. L. Boivin, M. A. Mahdavi, and R. E. Nygren
- 10F126 **Spectral measurements of runaway electrons by a scanning probe in the TEXTOR tokamak** (3 pages)
T. Kudyakov, K. H. Finken, M. Jakubowski, M. Lehnen, Y. Xu, and O. Willi
- 10F127 **Probes for measuring fluctuation-induced Maxwell and Reynolds stresses in the edge of the Madison Symmetric Torus reversed field pinch** (3 pages)
A. Kuritsyn, G. Fiksel, M. C. Miller, A. F. Almagri, M. Reyfman, and J. S. Sarff
- 10F128 **Triple probe signal detection electronics for systems lacking a well defined ground** (4 pages)
R. Compeau, M. Gilmore, and C. Watts
- 10F129 **A three dimensional probe positioner** (2 pages)
T. Intrator, X. Sun, L. Dorf, I. Furno, and G. Lapenta

DIAGNOSTIC SUITES, HARSH ENVIRONMENTS, NEUTRAL BEAMS, ION
BEAMS, PELLET INJECTION, DATA ACQUISITION AND ANALYSIS,
ENGINEERING, AND DUST MEASUREMENTS—*RÉJEAN L. BOIVIN*,
SESSION CHAIRMAN

- 10F301 **Diagnostics hardening for harsh environment in Laser Mégajoule (invited)**
(8 pages)
J. L. Bourgade, R. Marmoret, S. Darbon, R. Rosch, P. Troussel,
B. Villette, V. Glebov, W. T. Shmayda, J. C. Gomme,
Y. Le Tonqueze, F. Aubard, J. Baggio, S. Bazzoli, F. Bonneau,
J. Y. Boutin, T. Caillaud, C. Chollet, P. Combis, L. Disdier,
J. Gazave, S. Girard, D. Gontier, P. Jaanimagi, H. P. Jacquet,
J. P. Jadaud, O. Landoas, J. Legendre, J. L. Leray, R. Maroni,
D. D. Meyerhofer, J. L. Miquel, F. J. Marshall, I. Masclet-Gobin,
G. Pien, J. Raimbourg, C. Reverdin, A. Richard,
D. Rubin de Cervens, C. T. Sangster, J. P. Seaux, G. Soullie,
C. Stoeckl, I. Thfoin, L. Videau, and C. Zuber
- 10F302 **Diagnostics for fast ignition science (invited)** (5 pages)
A. G. MacPhee, K. U. Akli, F. N. Beg, C. D. Chen, H. Chen,
R. Clarke, D. S. Hey, R. R. Freeman, A. J. Kemp, M. H. Key,
J. A. King, S. Le Pape, A. Link, T. Y. Ma, H. Nakamura,
D. T. Offermann, V. M. Ovchinnikov, P. K. Patel, T. W. Phillips,
R. B. Stephens, R. Town, Y. Y. Tsui, M. S. Wei, L. D. Van Woerkom,
and A. J. Mackinnon
- 10F303 **Dust measurements in tokamaks (invited)** (6 pages)
D. L. Rudakov, J. H. Yu, J. A. Boedo, E. M. Hollmann,
S. I. Krasheninnikov, R. A. Moyer, S. H. Muller, A. Yu. Pigarov,
M. Rosenberg, R. D. Smirnov, W. P. West, R. L. Boivin, B. D. Bray,
N. H. Brooks, A. W. Hyatt, C. P. C. Wong, A. L. Roquemore,
C. H. Skinner, W. M. Solomon, S. Ratynskaia,
M. E. Fenstermacher, M. Groth, C. J. Lasnier, A. G. McLean,
and P. C. Stangeby
- 10F304 **Diagnostic components in harsh radiation environments: Possible overlap in
R&D requirements of inertial confinement and magnetic fusion systems**
(5 pages)
J. L. Bourgade, A. E. Costley, R. Reichle, E. R. Hodgson,
W. Hsing, V. Glebov, M. Decreton, R. Leeper, J. L. Leray,
M. Dentan, T. Hutter, A. Moroño, D. Eder, W. Shmayda, B. Brichard,
J. Baggio, L. Bertalot, G. Vayakis, M. Moran, T. C. Sangster,
L. Vermeeren, C. Stoeckl, S. Girard, and G. Pien
- 10F305 **TRIDENT high-energy-density facility experimental capabilities and diagnostics**
(3 pages)
S. H. Batha, R. Aragonéz, F. L. Archuleta, T. N. Archuleta,
J. F. Benage, J. A. Cobble, J. S. Cowan, V. E. Fatherley,
K. A. Flippo, D. C. Gautier, R. P. Gonzales, S. R. Greenfield,
B. M. Hegelich, T. R. Hurry, R. P. Johnson, J. L. Kline,
S. A. Letzring, E. N. Loomis, F. E. Lopez, S. N. Luo,
D. S. Montgomery, J. A. Oertel, D. L. Paisley, S. M. Reid,
P. G. Sanchez, A. Seifter, T. Shimada, and J. B. Workman
- 10F306 **Two dimensional radiated power diagnostics on Alcator C-Mod** (4 pages)
M. L. Reinke and I. H. Hutchinson

(Continued)

- 10F307 **The diagnostic system of the neutral beam injectors for ITER heating and current drive** (4 pages)
Gianluigi Serianni, Nicola Pomaro, Roberto Pasqualotto,
Monica Spolaore, and Marco Valisa
- 10F308 **Upgrade of the analyzer design for multipoint measurements by a gold neutral beam probe on the GAMMA 10 tandem mirror** (3 pages)
Y. Miyata, M. Yoshikawa, Y. Oono, M. Mizuguchi, Y. Nakashima,
S. Goshu, M. Nakada, and T. Imai
- 10F309 **Study of radial potential fluctuations by using a gold neutral beam probe system** (3 pages)
M. Mizuguchi, M. Yoshikawa, Y. Miyata, S. Goshu, M. Nakada,
Y. Oono, Y. Nakashima, and T. Imai
- 10F310 **An analysis of the influence of impurities on fast particle attenuation and on fast ion spectral shape in LHD** (3 pages)
Evgeny A. Veshchev, Pavel R. Goncharov, Tetsuo Ozaki,
and Shigeru Sudo
- 10F311 **Analysis of anisotropic suprathermal ion distributions using multidirectional measurements of escaping neutral atom fluxes** (3 pages)
P. R. Goncharov, T. Ozaki, E. A. Veshchev, and S. Sudo
- 10F312 **Calculation of low-Z impurity pellet induced fluxes of charge exchange neutral particles escaping from magnetically confined toroidal plasmas** (3 pages)
P. R. Goncharov, T. Ozaki, S. Sudo, N. Tamura, I. Yu. Tolstikhina,
and V. Yu. Sergeev
- 10F313 **Time-of-flight neutral particle analyzer and calibration** (5 pages)
W. S. Harris, E. P. Garate, W. W. Heidbrink, R. McWilliams,
T. Roche, E. Trask, and Yang Zhang
- 10F314 **Comparison of gridded energy analyzer and laser induced fluorescence measurements of a two-component ion distribution** (3 pages)
Z. Harvey, S. Chakraborty Thakur, A. Hansen, R. Hardin,
W. S. Przybysz, and E. E. Scime
- 10F315 **Compact, accurate description of diagnostic neutral beam propagation and attenuation in a high temperature plasma for charge exchange recombination spectroscopy analysis** (4 pages)
Igor O. Bepamyatnov, William L. Rowan, and Robert S. Granetz
- 10F316 **Effects of filament geometry on the arc efficiency of a high-intensity He⁺ ion source** (3 pages)
T. Kobuchi, M. Kisaki, K. Shinto, A. Okamoto, S. Kitajima,
M. Sasao, K. Tsumori, O. Kaneko, H. Sakakita, S. Kiyama,
Y. Hirano, and M. Wada
- 10F317 **Magnetic field fluctuation measurement with a heavy ion beam probe in the Large Helical Device** (3 pages)
A. Shimizu, T. Ido, M. Nishiura, H. Nakano, and S. Ohshima
- 10F318 **Measurement of electrostatic potential fluctuation using heavy ion beam probe in large helical device** (4 pages)
Takeshi Ido, Akihiro Shimizu, Masaki Nishiura, Haruhisa Nakano,
Shinsuke Ohshima, Shinji Kato, Yasuji Hamada, Yasuo Yoshimura,
Shin Kubo, Takashi Shimosuma, Hiroe Igami, Hiromi Takahashi,
Kazuo Toi, and Fumitake Watanabe

(Continued)

- 10F319 **Observation of plasma density fluctuations by a heavy ion beam probe diagnostic with multiple cell array detector on the tokamak ISTTOK** (3 pages)
I. S. Nedzelskiy, R. Coelho, D. Alves, C. Silva, and H. Fernandes
- 10F320 **Measurements of spatial structure of plasma potential and density fluctuations by multichannel heavy ion beam probe on large helical device** (3 pages)
Shinsuke Ohshima, Takeshi Ido, Akihiro Shimizu, Masaki Nishiura, and Haruhisa Nakano
- 10F321 **A compact flexible pellet injector for the TJ-II stellarator** (3 pages)
K. J. McCarthy, S. K. Combs, L. R. Baylor, J. B. O. Caughman, D. T. Fehling, C. R. Foust, J. M. McGill, J. M. Carmona, and D. A. Rasmussen
- 10F322 **Radiation flux and spectral analysis of the multi-temperature Z dynamic hohlraum** (5 pages)
T. E. Lockard, G. C. Idzorek, T. E. Tierney, IV, and R. G. Watt
- 10F323 **Different methods of reconstructing spectra from filtered x-ray diode measurements** (4 pages)
Achim Seifter and George A. Kyrala
- 10F324 **Forward modeling of JET polarimetry diagnostic** (3 pages)
Oliver Ford, J. Svensson, A. Boboc, D. C. McDonald, and JET-EFDA Contributors
- 10F325 **Accuracy of EFIT equilibrium reconstruction with internal diagnostic information at JET** (4 pages)
M. Brix, N. C. Hawkes, A. Boboc, V. Drozdov, S. E. Sharapov, and JET-EFDA Contributors
- 10F326 **Classifier based on support vector machine for JET plasma configurations** (3 pages)
S. Dormido-Canto, G. Farias, J. Vega, R. Dormido, J. Sánchez, N. Duro, H. Vargas, A. Murari, and JET-EFDA Contributors
- 10F327 **Intelligent technique to search for patterns within images in massive databases** (3 pages)
J. Vega, A. Murari, A. Pereira, A. Portas, P. Castro, and JET-EFDA Contributors
- 10F328 **Feature extraction for improved disruption prediction analysis at JET** (3 pages)
G. A. Rattá, J. Vega, A. Murari, M. Johnson, and JET-EFDA Contributors
- 10F329 **Real-time plasma control based on the ISTTOK tomography diagnostic** (3 pages)
P. J. Carvalho, B. B. Carvalho, A. Neto, R. Coelho, H. Fernandes, J. Sousa, C. Varandas, E. Chávez-Alarcón, and J. J. E. Herrera-Velázquez
- 10F330 **Filterscopes: Spectral line monitors for long-pulse plasma devices** (4 pages)
N. H. Brooks, R. J. Colchin, D. T. Fehling, D. L. Hillis, Y. Mu, and E. Unterberg
- 10F331 **Using Cramer–Rao theory as spectrometer design tool aimed at quantitative complex-spectrum analysis** (3 pages)
J. F. F. Klinkhamer, N. C. J. van der Valk, M. G. von Hellermann, and R. Jaspers

(Continued)

- 10F332 **Development of a reconstruction procedure for the halo current distribution** (4 pages)
Edoardo Alessi, M. Cavinato, and G. Chitarin
- 10F333 **Dust as a versatile matter for high-temperature plasma diagnostic** (3 pages)
Zhehui Wang and Catalin M. Ticos
- 10F334 **Three-dimensional reconstruction of dust particle trajectories in the NSTX** (4 pages)
W. U. Boeglin, A. L. Roquemore, and R. Maqueda
- 10F335 **Implementation of local area network extension for instrumentation standard trigger capabilities in advanced data acquisition platforms** (4 pages)
J. M. López, M. Ruiz, E. Barrera, G. de Arcas, and J. Vega
- 10F336 **Self-adaptive sampling rate data acquisition in JET's correlation reflectometer** (4 pages)
G. de Arcas, J. M. López, M. Ruiz, E. Barrera, J. Vega, A. Murari, A. Fonseca, and JET-EFDA Contributors
- 10F337 **Diagnostic developments for quasicontinuous operation of the Wendelstein 7-X stellarator** (4 pages)
R. König, J. Cantarini, H. Dreier, V. Erckmann, D. Hildebrandt, M. Hirsch, G. Kocsis, P. Kornejew, M. Laux, H. Laqua, E. Pasch, S. Recsei, V. Szabó, H. Thomsen, A. Weller, A. Werner, R. Wolf, M. Y. Ye, and S. Zoletnik
- 10F338 **In situ window cleaning by laser blowoff through optical fiber** (4 pages)
A. Alfier, S. Barison, T. Danieli, L. Giudicotti, C. Pagura, and R. Pasqualotto
- OPTICAL (IR, VISIBLE, UV, EUV), MOTIONAL STARK EFFECT, CHARGE EXCHANGE, RECOMBINATION, BEAM EMISSION SPECTROSCOPY, OPTICAL SPECTROSCOPY, AND SUPRATHERMAL ELECTRONS—BRENTLEY STRATTON, SESSION CHAIRMAN
- 10F501 **Diagnostic techniques for measuring suprathermal electron dynamics in plasmas (invited)** (8 pages)
S. Coda
- 10F502 **A novel compact high speed x-ray streak camera (invited)** (4 pages)
J. D. Hares and A. K. L. Dymoke-Bradshaw
- 10F503 **A high-resolution coherent transition radiation diagnostic for laser-produced electron transport studies (invited)** (5 pages)
M. Storm, I. A. Begishev, R. J. Brown, C. Guo, D. D. Meyerhofer, C. Mileham, J. F. Myatt, P. M. Nilson, T. C. Sangster, C. Stoeckl, W. Theobald, and J. D. Zuegel
- 10F504 **Suprathermal electron studies in the TCV tokamak: Design of a tomographic hard-x-ray spectrometer** (5 pages)
S. Gnesin, S. Coda, J. Decker, and Y. Peysson
- 10F505 **Use of Cherenkov-type detectors for measurements of runaway electrons in the ISTTOK tokamak** (5 pages)
V. V. Plyusnin, L. Jakubowski, J. Zebrowski, H. Fernandes, C. Silva, K. Malinowski, P. Duarte, M. Rabinski, and M. J. Sadowski
- 10F506 **Imaging photomultiplier array with integrated amplifiers and high-speed USB interface** (3 pages)
M. Blacksell, J. Wach, D. Anderson, J. Howard, S. M. Collis, B. D. Blackwell, D. Andruczyk, and B. W. James

(Continued)

- 10F507 **Detection of a new parametric decay instability branch in TST-2 during high harmonic fast wave heating** (3 pages)
Y. Adachi, A. Ejiri, Y. Takase, O. Watanabe, T. Oosako, H. Tojo, S. Kainaga, T. Masuda, M. Sasaki, J. Sugiyama, and T. Yamaguchi
- 10F508 **Fast visible imaging of turbulent plasma in TORPEX** (4 pages)
D. Iraj, A. Diallo, A. Fasoli, I. Furno, and S. Shibaev
- 10F509 **Progress of the ITER equatorial vis/IR wide angle viewing system optical design** (3 pages)
M. Davi, Y. Corre, D. Guilhem, F. Jullien, R. Reichle, S. Salasca, J. M. Travère, E. de la Cal, A. Manzanares, J. L. de Pablos, and J. B. Migozzi
- 10F510 **Installation of a fast framing visible camera on KSTAR** (3 pages)
Jinil Chung, Deok Kyo Lee, Dongcheol Seo, and Myoung Choul Choi
- 10F511 **The ITER bolometer diagnostic: Status and plans** (5 pages)
H. Meister, L. Giannone, L. D. Horton, G. Raupp, W. Zeidner, G. Grunda, S. Kalvin, U. Fischer, A. Serikov, S. Stickel, and R. Reichle
- 10F512 **Development of a virtual Z_{eff} diagnostic for the W7-X stellarator** (4 pages)
M. Krychowiak, D. Dodt, H. Dreier, R. König, and R. Wolf
- 10F513 **Optical design study of an infrared visible viewing system for Wendelstein 7-X divertor observation and control** (4 pages)
J. Cantarini, D. Hildebrandt, R. König, F. Klinkhamer, K. Moddemeijer, W. Vliegthart, and R. Wolf
- 10F514 **Development of a phase contrast imaging system based on a yttrium aluminum garnet laser with folded beam for observations of density fluctuations in compact helical system** (4 pages)
K. Matsuo, N. Uchida, M. Kawakubo, H. Iguchi, S. Okamura, K. Matsuoka, and T. Akiyama
- 10F515 **Heat flow diagnostics for helicon plasmas** (3 pages)
Daniel F. Berisford, Roger D. Bengtson, Laxminarayan L. Raja, Leonard D. Cassady, and William J. Chancery
- 10F516 **Spectrally filtered fast imaging of internal magnetohydrodynamic activity in the DIII-D tokamak** (4 pages)
J. H. Yu and M. A. Van Zeeland
- 10F517 **Measurements of the internal magnetic field on DIII-D using intensity and spacing of the motional Stark multiplet** (4 pages)
N. A. Pablant, K. H. Burrell, R. J. Groebner, D. H. Kaplan, and C. T. Holcomb
- 10F518 **Overview of equilibrium reconstruction on DIII-D using new measurements from an expanded motional Stark effect diagnostic** (4 pages)
C. T. Holcomb, M. A. Makowski, S. L. Allen, W. H. Meyer, and M. A. Van Zeeland
- 10F519 **Optimization of the optical design of the ITER MSE diagnostic** (4 pages)
M. A. Makowski, S. L. Allen, C. T. Holcomb, S. Lerner, K. Morris, and N. Wong
- 10F520 **Design of a new optical system for Alcator C-Mod motional Stark effect diagnostic** (4 pages)
Jinseok Ko, Steve Scott, Manfred Bitter, and Scott Lerner

(Continued)

- 10F521 **The motional Stark effect diagnostic for ITER using a line-shift approach**
(4 pages)
E. L. Foley, F. M. Levinton, H. Y. Yuh, and L. E. Zakharov
- 10F522 **The motional Stark effect diagnostic on NSTX** (5 pages)
F. M. Levinton and H. Yuh
- 10F523 **Simulation of the motional Stark effect diagnostic gas-filled torus calibration**
(4 pages)
Howard Y. Yuh, F. M. Levinton, S. D. Scott, and J. Ko
- 10F524 **Ab initio modeling of the motional Stark effect on MAST** (5 pages)
M. F. M. De Bock, N. J. Conway, M. J. Walsh, P. G. Carolan,
and N. C. Hawkes
- 10F525 **Impact of calibration technique on measurement accuracy for the JET core charge-exchange system** (5 pages)
Carine Giroud, A. G. Meigs, C. R. Negus, K.-D. Zastrow,
T. M. Biewer, T. W. Versloot, and JET-EFDA Contributors
- 10F526 **Validation of the ITER CXRS design by tests on TEXTOR** (4 pages)
R. J. E. Jaspers, M. G. von Hellermann, E. Delabie, W. Biel,
O. Marchuk, and L. Yao
- 10F527 **Modeling the effect of reflection from metallic walls on spectroscopic measurements** (4 pages)
K.-D. Zastrow, S. R. Keatings, L. Marot, M. G. O'Mullane,
G. de Temmerman, and JET-EFDA Contributors
- 10F528 **Ultrafast ion temperature and toroidal velocity fluctuation spectroscopy diagnostic design** (4 pages)
G. R. McKee, D. J. Schlossberg, and M. W. Shafer
- 10F529 **Wide-view charge exchange recombination spectroscopy diagnostic for Alcator C-Mod** (4 pages)
W. L. Rowan, I. O. Bespamyatnov, and R. S. Granetz
- 10F530 **A proposed in-vessel calibration light source for the Joint European Torus**
(3 pages)
T. M. Biewer, D. L. Hillis, M. F. Stamp, K.-D. Zastrow,
and JET-EFDA Contributors
- 10F531 **Characterization of cross-section correction to charge exchange recombination spectroscopy rotation measurements using co- and counter-neutral-beam views** (4 pages)
W. M. Solomon, K. H. Burrell, R. Feder, A. Nagy, P. Gohil,
and R. J. Groebner
- 10F532 **Review of atomic data needs for active charge-exchange spectroscopy on ITER** (3 pages)
O. Marchuk, G. Bertschinger, W. Biel, E. Delabie,
M. G. von Hellermann, R. Jaspers, and D. Reiter
- 10F533 **Magnetic fluctuation profile measurement using optics of motional Stark effect diagnostics in JT-60U** (5 pages)
T. Suzuki, A. Isayama, G. Matsunaga, N. Oyama, T. Fujita,
and T. Oikawa
- 10F534 **Singular value decomposition filtering for enhanced signal extraction from two-dimensional beam emission spectroscopy measurements** (4 pages)
M. W. Shafer, G. R. McKee, and D. J. Schlossberg

(Continued)

- 10F535 **An ion Doppler spectrometer instrument for ion temperature and flow measurements on SSPX** (4 pages)
J. D. King, H. S. McLean, R. D. Wood, C. A. Romero-Talamás, J. M. Moller, and E. C. Morse
- 10F536 **Z_{eff} profile measurement system with an optimized Czerny–Turner visible spectrometer in large helical device** (3 pages)
H. Y. Zhou, S. Morita, M. Goto, and M. B. Chowdhuri
- 10F537 **Spectroscopic evaluation of three different gratings used for a flat-field extreme ultraviolet spectrometer to monitor $\Delta n=1$ transitions from medium-Z impurities in 10–30 Å** (3 pages)
Malay Bikas Chowdhuri, Shigeru Morita, Motoshi Goto, and Hiroyuki Sasai
- 10F538 **Grazing-incidence spectrometer on the SSPX spheromak** (3 pages)
J. Clementson, P. Beiersdorfer, and E. W. Magee
- 10F539 **Near-infrared spectroscopy for burning plasma diagnostic applications** (5 pages)
V. A. Soukhanovskii
- 10F540 **An experimental system for spectral line ratio measurements in the TJ-II stellarator** (4 pages)
B. Zurro, A. Baciero, J. M. Fontdecaba, R. Peláez, and D. Jiménez-Rey
- 10F541 **Spectroscopic diagnostics for ablation cloud of tracer-encapsulated solid pellet in LHD** (4 pages)
N. Tamura, V. Yu. Sergeev, D. V. Kalinina, I. V. Miroshnikov, K. Sato, I. A. Sharov, O. A. Bakhareva, D. M. Ivanova, V. M. Timokhin, S. Sudo, and B. V. Kuteev
- 10F542 **Extreme ultraviolet spectroscopy diagnostics of low-temperature plasmas based on a sliced multilayer grating and glass capillary optics** (5 pages)
V. L. Kantsyrev, A. S. Safronova, K. M. Williamson, P. Wilcox, N. D. Quart, M. F. Yilmaz, K. W. Struve, D. L. Voronov, R. M. Feshchenko, I. A. Artyukov, and A. V. Vinogradov
- 10F543 **Extreme ultraviolet spectroscopy of low-Z ion plasmas for fusion applications** (3 pages)
P. G. Wilcox, A. S. Safronova, V. L. Kantsyrev, U. I. Safronova, K. M. Williamson, M. F. Yilmaz, J. Clementson, P. Beiersdorfer, and K. W. Struve
- 10F544 **Multichannel Doppler transmission grating spectrometer at the Alcator C-Mod tokamak** (3 pages)
A. Graf, M. May, and P. Beiersdorfer
- 10F545 **Temporal dispersion of a spectrometer** (4 pages)
A. Visco, R. P. Drake, D. H. Froula, S. H. Glenzer, and B. B. Pollock
- 10F546 **Reliable and repeatable characterization of optical streak cameras** (5 pages)
Michael R. Charest, Jr., Peter Torres, III, Christopher T. Silbernegel, and Daniel H. Kalantar
- 10F547 **A novel backscatter focus diagnostic for the TRIDENT 200 TW laser** (2 pages)
D. C. Gautier, K. A. Flippo, S. A. Letzring, J. Workman T. Shimada, R. P. Johnson, T. R. Hurry, S. A. Gaillard, and B. M. Hegelich

(Continued)

- 10F548 **A pulsed-laser calibration system for the laser backscatter diagnostics at the Omega laser** (3 pages)
Paul Neumayer, Charles Sorce, Dustin H. Froula, Laurent Divol,
Vern Rekow, Kevin Loughman, Russel Knight,
Siegfried H. Glenzer, Raymond Bahr, and Wolf Seka
- 10F549 **Optical transmission of glass for the National Ignition Facility near backscatter imagers under x-ray exposure** (4 pages)
R. A. London, D. H. Froula, C. M. Sorce, J. D. Moody, L. J. Suter,
S. H. Glenzer, O. S. Jones, N. B. Meezan, and M. D. Rosen
- 10F550 **Multicentimeter long high density magnetic plasmas for optical guiding** (3 pages)
B. B. Pollock, D. H. Froula, G. R. Tynan, L. Divol, D. Price,
R. Costa, F. Yepiz, S. Fulkerson, F. Mangini, and S. H. Glenzer
- 10F551 **Using a short-pulse diffraction-limited laser beam to probe filamentation of a random phase plate smoothed beam** (3 pages)
J. L. Kline, D. S. Montgomery, K. A. Flippo, R. P. Johnson,
H. A. Rose, T. Shimada, and E. A. Williams

ADDENDA

- 10F701 **Addendum to papers from Joint European Torus-European Fusion Development Agreement (JET-EFDA) Contributors, published in *Proceedings of the 17th Topical Conference on High-Temperature Plasma Diagnostics, Albuquerque, New Mexico, May 2008*** (5 pages)
Albert T. Macrander *Editor*
- A1 **CUMULATIVE AUTHOR INDEX** (5 pages)

A method to measure the frequencies of individual half cells in a dumbbell cavity

Sun An,^{1,a)} Zhang Liping,^{1,2} Tang Yazhe,¹ Ying-min Li,¹ and Yong-Sub Cho¹

¹PEFP, Korea Atomic Energy Research Institute, Daejeon 305-353, Republic of Korea

²Construction Machinery School, Chang'an University, Xi'an 710064, People's Republic of China

(Received 22 April 2008; accepted 31 August 2008; published online 7 October 2008)

Dumbbell fabrication is a midprocess for manufacturing an elliptical superconducting rf cavity. In order to understand how a welding shrinkage affects a dumbbell's frequencies and length, we need to measure the exact frequencies of each individual half cell of a dumbbell. To improve such a calculation precision and to simplify the calculation formulae, based on a two-coupled oscillator model and a cavity perturbation theory, a new formula to calculate the individual half-cell frequencies of a dumbbell or the individual cavity frequencies of a two-cavity coupling system has been developed, and its performance has been confirmed by using a dumbbell simulation. This formula can be applied to any kind of rf cavities with electric, magnetic, or electromagnetic coupling, if a coupling hole between two coupling cavities is small compared to the wavelength. Compared to other calculation formulae, this formula simplifies the calculation process of the individual resonator frequencies of a coupling system considerably, and it can also improve the calculation precision than that of a normal calculation method. Another advantage of this new method is that we do not need to consider a coupling factor between two resonators during a testing for an individual resonator frequency of an oscillator. The developed formula has been successfully used to tune the PEPF dumbbells. © 2008 American Institute of Physics.

[DOI: [10.1063/1.2987686](https://doi.org/10.1063/1.2987686)]

I. INTRODUCTION

At present, a superconducting rf (SRF) accelerator is part of the accelerating structure of new particle accelerators.¹⁻⁶ For a SRF elliptical cavity accelerator, a TM010 π mode electric field is used to accelerate a charged particle. Control of the cavity frequency and field flatness of the TM010 π mode is very important during a SRF cavity production.⁷

Based on the present technology, a dumbbell fabrication is a necessary midprocess for a SRF cavity manufacture. Normally, the two half cells are welded at their irises to become a primary dumbbell. After that, a stiffening ring (single or double) is welded between these two half cells, on their outer wall. Due to a stiffening-ring welding shrinkage, the frequencies and the lengths of the two individual half cells become different, and also, the electric fields become nonsymmetric in the two half cells.

A dumbbell with a right length and frequency is necessary to build up a desired cavity. PEPF low-beta dumbbell has a double stiffening-ring structure.⁸⁻¹² In order to know how a stiffening-ring welding shrinkage affects the frequencies and how difficult it will be to tune the length and frequency of the individual half cells of a PEPF dumbbell, we need to know the exact TM010 π mode frequency of the individual half cells.

In order to measure the TM010 π mode frequency of the individual half cells precisely, first we used a simulation result to confirm the existing calculation method, which can be used to calculate an individual half cell's frequency. After checking the existing methods described in Refs. 13 and 14 we found that the calculation method was too complicated, and the precision of the method could not meet our measurement requirements; with the same methods it is not easy to obtain a consistent result. Then based on a two-coupled oscillator model and a cavity perturbation theory, a new formula to calculate the individual half-cell frequencies of a dumbbell or the individual cavity frequencies of a two-cavity coupling system has been developed and its performance has been confirmed by using a dumbbell simulation. The new formula is much simpler and easier to use than others. Finally, the new method is successfully used to tune the PEPF low-beta dumbbells.

II. VERIFICATION OF THE EXISTING MEASUREMENT METHODS TO MEASURE THE INDIVIDUAL HALF CELLS' FREQUENCIES OF A DUMBBELL

Normally, a perturbation method is used to measure the frequencies of the individual half cells in a dumbbell. A dumbbell with shorted ends or two metal plates is a resonator.¹⁵ We installed two small antennas on the plates and used a network analyzer to measure the dumbbell frequencies of the TM010 $\pi/2$ and π modes: $f_{\pi/2}$ and f_{π} , as shown in Fig. 1. A perturbation plate with an antenna and a short metal stick is used to measure the perturbed dumbbell frequencies of the TM010 $\pi/2$ and π modes (see Fig. 2).

^{a)}Present address: Proton Engineering Frontier Project, Korea Atomic Energy Research Institute, Daejeon 305-353, Republic of Korea. Tel.: _82-42-868-2975. FAX: _82-42-861-6950. Electronic mail: sunan@kaeri.re.kr.

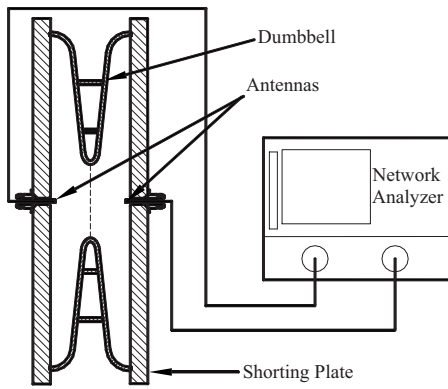


FIG. 1. A sketch of the frequency measurement setup for a PEFP low-beta dumbbell.

Alternating the positions between the plates with and without a tip, we obtain the frequency shifts of the $TM_{010} \pi/2$ and π modes of the individual half cells due to a perturbation. According to the tested frequencies of a dumbbell, the individual half-cell frequencies are obtained by using formulae, which can provide the individual half-cell frequencies. For a dumbbell cavity, here we use subscript “ l ” to indicate the physical parameters of the left half cell, and subscript r to indicate the physical parameters of the right half cell. The $f_{l,\pi}$ and $f_{r,\pi}$ describe the frequencies of the half cells simulated by POISSON SUPERFISH (Ref. 16) with such a boundary: the iris side is magnetic, and the equator side is electric. The simulated boundaries for frequencies $f_{l,\pi/2}$ and $f_{r,\pi/2}$ of the half cells are that both the iris side and the equator are electric. $f_{p,l,\pi}$ and $f_{p,l,\pi/2}$ are the TM_{010} passbands of the dumbbell with the tip on the left half-cell side; and $f_{p,r,\pi}$ and $f_{p,r,\pi/2}$ are the TM_{010} passbands of the dumbbell with the tip on the right half-cell side.

There are several formulae used to calculate the frequencies of individual half cells.^{13,14} In order to confirm that these formulae can be used to calculate the half-cell frequencies precisely, we used CST MICROWAVE STUDIO (Ref. 17) to simulate an asymmetric dumbbell, as shown in Fig. 3. Here we used two PEFP low-beta half cells with different extra lengths at their equator to build a dumbbell: the extra length of the left half cell is 1.0 mm, and the extra length of the right half cell is 0.6 mm. The length and $TM_{010} \pi$ mode frequency of a normal PEFP low-beta half cell are 45.0 mm and 700.095 MHz, respectively, simulated by CST MICROWAVE STUDIO. A metal cylinder with a diameter of 2.0 mm

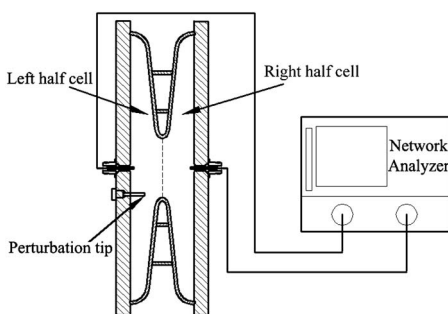


FIG. 2. A sketch of the perturbation measurement setup for a PEFP low-beta dumbbell.

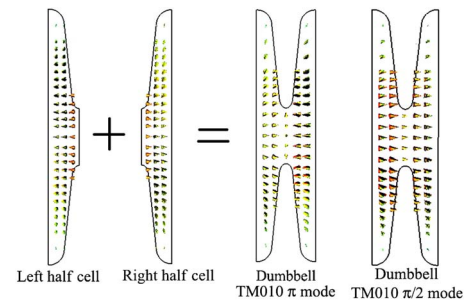


FIG. 3. (Color online) $TM_{010} \pi$ mode field distributions of a left half cell, a right half cell; and the $TM_{010} \pi$ and $\pi/2$ mode field distributions of a dumbbell combined by these two half-cells simulated by CST MICROWAVE STUDIO.

and a length of 5.0 mm as a perturbation tip is located either on a left half cell’s wall [see Fig. 4(a)] or on a right half cell’s wall [see Fig. 4(b)] near the dumbbell axis. Table I lists the simulation results by CST MICROWAVE STUDIO. In order to verify the accuracy of the simulation results, we confirmed the results by using POISSON SUPERFISH.

Submitting the simulated frequencies of the dumbbell with and without a perturbation body into the calculation method described by Ref. 13, we obtained the $TM_{010} \pi$ mode frequencies of the individual half cells: 697.510 MHz for the left half cell, and 698.129 MHz for the right half cell. The errors are 0.789 and 0.089 MHz for the left and right half cells, respectively. We think this calculation method is too complicated and the precision of the calculation formula cannot meet our measurement requirements. Another formula described in Ref. 15 is more complicated than this one, and it is not easy to obtain similar results. In order to improve the precision for a calculation and to simplify the calculation formulae, we decided to develop a new formula.

III. DEVELOPMENT OF A NEW FORMULA TO CALCULATE THE FREQUENCIES OF THE INDIVIDUAL HALF CELLS OF A DUMBBELL

Because we only consider the half-cell frequencies, here the cavity wall loss can be neglected. According to the theory for a diffraction by a small hole (the coupling hole is small compared to the wavelength), if the difference of the $TM_{010} \pi$ mode frequencies of the two individual half cells is not too

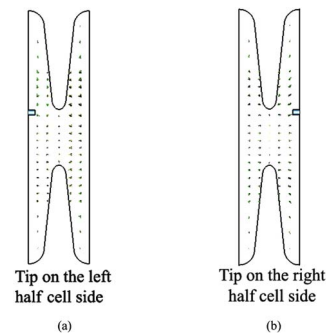


FIG. 4. (Color online) $TM_{010} \pi$ mode field distributions of a dumbbell for different tip positions simulated by CST MICROWAVE STUDIO.

TABLE I. A simulated dumbbell based on the PEFP low-beta middle half cells.

Resonator type	Length (mm)	Frequencies of TM010 mode (MHz)	
Normal half cell	45.00	f_π	700.095
Left half cell	46.0	$f_{l,\pi}$	696.721
Right half cell	45.6	$f_{r,\pi}$	698.041
Dumbbell	91.6	f_π	697.422
		$f_{\pi/2}$	687.463
Dumbbell with tip on the left half-cell side	91.6	$f_{p,l,\pi}$	697.341
		$f_{p,l,\pi/2}$	687.277
Dumbbell with tip on the right half-cell side	91.6	$f_{p,r,\pi}$	697.312
		$f_{p,r,\pi/2}$	687.306

large, namely, $f_{l,\pi} \approx f_{r,\pi} \approx f_{0,\pi}$, the frequencies and fields of the two half cells can be described by two-coupled oscillators without a energy loss¹⁸

$$\frac{d^2 E_l}{dt^2} + (2\pi f_{l,\pi})^2 E_l = (2\pi f_{0,\pi})^2 k(E_l - E_r),$$

$$\frac{d^2 E_r}{dt^2} + (2\pi f_{r,\pi})^2 E_r = (2\pi f_{0,\pi})^2 k(E_r - E_l). \quad (1)$$

Here k is a coupling factor between the half cells, and can be electric, magnetic, or both. E_l and E_r are the electrical fields of the TM010 modes in the left half cell and in the right half cell, respectively. At a stable resonant state E_l and E_r can be expressed as

$$E_l = E_{0l} \exp(-i2\pi ft),$$

$$E_r = E_{0r} \exp(-i2\pi ft). \quad (2)$$

Here f is either the frequency of the TM010 π or the $\pi/2$ mode. E_{0l} and E_{0r} are the electrical field amplitudes of E_l and E_r , respectively. Submitting Eq. (2) into Eq. (1), Eq. (1) becomes

$$(f^2 + f_{0,\pi}^2 k - f_{l,\pi}^2) E_{0l} = f_{0,\pi}^2 k E_{0r},$$

$$(f^2 + f_{0,\pi}^2 k - f_{r,\pi}^2) E_{0r} = f_{0,\pi}^2 k E_{0l}. \quad (3)$$

From Eq. (3), we obtain

$$\frac{f^2 + f_{0,\pi}^2 k - f_{l,\pi}^2}{f_{0,\pi}^2 k} = \frac{f_{0,\pi}^2 k}{f^2 + f_{0,\pi}^2 k - f_{r,\pi}^2}. \quad (4)$$

Moreover the frequencies of the TM010 modes

$$f_\pi^2 = \frac{1}{2}(f_{l,\pi}^2 + f_{r,\pi}^2) - f_{0,\pi}^2 k + \frac{1}{2}\sqrt{(f_{l,\pi}^2 - f_{r,\pi}^2)^2 + 4f_{0,\pi}^4 k^2},$$

$$f_{\pi/2}^2 = \frac{1}{2}(f_{l,\pi}^2 + f_{r,\pi}^2) - f_{0,\pi}^2 k - \frac{1}{2}\sqrt{(f_{l,\pi}^2 - f_{r,\pi}^2)^2 + 4f_{0,\pi}^4 k^2}. \quad (5)$$

Combining Eqs. (3) and (5), we found

$$\begin{aligned} \frac{E_{0r,\pi}}{E_{0l,\pi}} &= \frac{f_\pi^2 + f_{0,\pi}^2 k - f_{l,\pi}^2}{f_{0,\pi}^2 k} \\ &= \frac{f_{r,\pi}^2 - f_{l,\pi}^2}{2f_{0,\pi}^2 k} + \sqrt{\frac{(f_{l,\pi}^2 - f_{r,\pi}^2)^2}{4f_{0,\pi}^4 k^2} + 1}, \\ \frac{E_{0r,\pi/2}}{E_{0l,\pi/2}} &= \frac{f_{\pi/2}^2 + f_{0,\pi}^2 k - f_{l,\pi}^2}{f_{0,\pi}^2 k} \\ &= \frac{f_{r,\pi}^2 - f_{l,\pi}^2}{2f_{0,\pi}^2 k} - \sqrt{\frac{(f_{l,\pi}^2 - f_{r,\pi}^2)^2}{4f_{0,\pi}^4 k^2} + 1}. \end{aligned} \quad (6)$$

From Eq. (6) we found that $E_{0r,\pi}/E_{0l,\pi} > 0$ and $E_{0r,\pi/2}/E_{0l,\pi/2} < 0$. This means that the electric field direction is out of the normal plane or into the normal plane of the shorting plates at the same time for the TM010 π mode; but for the TM010 $\pi/2$ mode, the electric field direction is that one is out of the normal plane and another is into the normal plane of the shorting plates at the same time.

Because the tip is located very near to a cell's axis, where mainly an electric field exists, for the TM010 modes, according to the Slater perturbation theorem, the frequency changes of a dumbbell are given by¹⁹ $(f_0^2 - f^2)/f_0^2 = 1.5 E_0^2 \epsilon_0 V/U$, in which V is the volume of the tip. f_0 and E_0 are the dumbbell frequency (TM010 π or $\pi/2$ mode) and the electric field at the tip position before a tip perturbation, respectively. f is the dumbbell frequency after the tip perturbs. U is the stored energy in the dumbbell. Noting that $E_{0r,\pi}/E_{0l,\pi} > 0$ and $E_{0r,\pi/2}/E_{0l,\pi/2} < 0$, we obtained

$$\begin{aligned} \frac{E_{0r,\pi}}{E_{0l,\pi}} &= \sqrt{\frac{f_\pi^2 - f_{p,r,\pi}^2}{f_\pi^2 - f_{p,l,\pi}^2}}, \\ \frac{E_{0r,\pi/2}}{E_{0l,\pi/2}} &= -\sqrt{\frac{f_{\pi/2}^2 - f_{p,r,\pi/2}^2}{f_{\pi/2}^2 - f_{p,l,\pi/2}^2}}. \end{aligned} \quad (7)$$

Combining this with Eqs. (5) and (6), we obtained the frequency calculation formulae for the individual half cells of a dumbbell

$$\begin{aligned} f_{l,\pi} &= \sqrt{\frac{f_\pi^2 + f_{\pi/2}^2}{2} + \frac{(f_\pi^2 - f_{\pi/2}^2)(2-R)}{2\sqrt{R+4}}}, \\ f_{r,\pi} &= \sqrt{\frac{f_\pi^2 + f_{\pi/2}^2}{2} + \frac{(f_\pi^2 - f_{\pi/2}^2)(2+R)}{2\sqrt{R+4}}}, \\ \text{here } R &= \sqrt{\frac{f_\pi^2 - f_{p,r,\pi}^2}{f_\pi^2 - f_{p,l,\pi}^2}} - \sqrt{\frac{f_{\pi/2}^2 - f_{p,r,\pi/2}^2}{f_{\pi/2}^2 - f_{p,l,\pi/2}^2}}. \end{aligned} \quad (8)$$

Submitting the data in Table I into Eq. (8), we found that the TM010 π mode frequency of the left half cell is 696.684

MHz, and the one for the right half cell is 697.868 MHz. Compared to the simulated $f_{l,\pi}$ and $f_{r,\pi}$, the errors are 0.037 and 0.173 MHz. By neglecting the errors introduced by the CST MICROWAVE STUDIO simulation, we assume that this calculation formula is simpler, and can improve the precision of a result by four times that calculated in Sec. II by using the calculation method in Ref. 13.

An accelerating mode's field flatness is an important parameter for a multicell cavity. For a dumbbell cavity, according to the definition of the field flatness,⁷ its field flatness can be expressed as

$$\eta_{ff} = \frac{|E_{0r,\pi} - E_{0l,\pi}|}{0.5(E_{0r,\pi} + E_{0l,\pi})} 100\%. \quad (9)$$

Combining this with Eq. (7), the dumbbell cavity's field flatness is

$$\eta_{ff} = \frac{|\sqrt{f_{\pi}^2 - f_{p,r,\pi}^2} - \sqrt{f_{\pi}^2 - f_{p,l,\pi}^2}|}{\sqrt{f_{\pi}^2 - f_{p,r,\pi}^2} + \sqrt{f_{\pi}^2 - f_{p,l,\pi}^2}} 200\%. \quad (10)$$

The dumbbell cavity's coupling coefficient¹³ can be obtained by

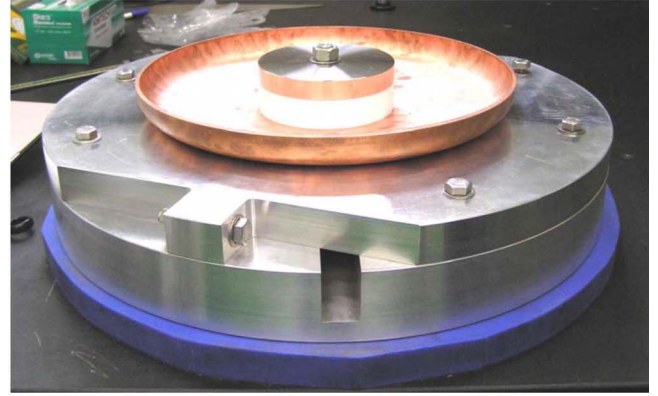
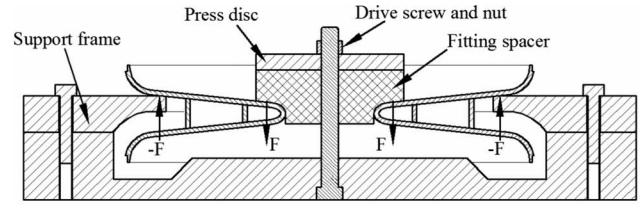
$$K = \frac{0.5(f_{\pi}^2 - f_{\pi/2}^2)}{2f_{\pi/2}^2 - f_{\pi}^2}. \quad (11)$$

The above formulae have shown that we can calculate an individual half cell's frequencies, and its field flatness by directly using a perturbation technique.

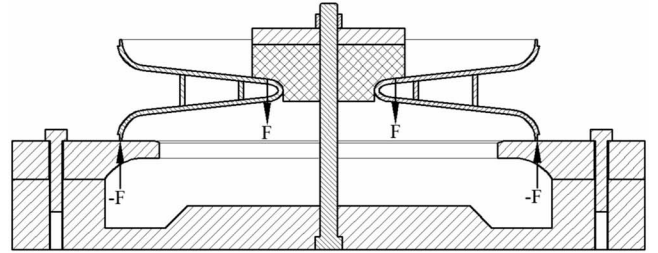
IV. PEFP DUMBBELL TUNING BY USING THE NEW FORMULA AND THE EXPERIMENTAL RESULTS

Before a PEFP low-beta dumbbell fabrication, each half-cell equator is 1.0 mm longer than the length determined by a SUPERFISH calculation for a dumbbell tuning and trimming, and each iris is trimmed to a suitable length by considering a welding shrinkage, then the two half cells are welded at their irises to become a primary dumbbell. After a single or double stiffening ring has been welded between two half cells, the primary dumbbell becomes a dumbbell for a SRF cavity fabrication. In order to measure and tune the PEFP low-beta dumbbells, a frequency measurement set and tuning set have been designed and fabricated. The PEFP dumbbell tuning set can stretch or press an individual half cell of a dumbbell. A spacer is used to press a half cell at its iris. A tuning ring can stretch or press a half cell at or around its equator, as shown in Fig. 5.

During the tuning of a dumbbell, the following procedure²⁰ is used. (1) Measure dumbbell's TM010 passbands f_{π} and $f_{\pi/2}$ by using a frequency testing set and a network analyzer (see Fig. 6). (2) Measure a dumbbell's length by a vernier caliper. (3) Test its perturbation frequencies $f_{p,l,\pi}$, $f_{p,l,\pi/2}$, $f_{p,r,\pi}$ and $f_{p,r,\pi/2}$ by using an asymmetrical frequency testing set and a network analyzer. (4) According to Eq. (8) obtain its individual half cells' frequencies; compare the target frequency and length with the measured frequency and length; and obtain the tuning frequencies or the trimming length: Δf_l and Δf_r . The trimming frequency sensitivity S_{trim} at an equator in a dumbbell's axial direction is obtained by a testing or by a simulation. The trimming



(a)



(b)

FIG. 5. (Color online) The sketches to tune the individual half cells and the PEFP tuning set. (a) Stretch a half cell and increase its TM010 π mode frequency; (b) press a half cell and decrease its TM010 π mode frequency.

lengths are $\Delta L_l = \Delta f_l / S_{\text{trim}}$ and $\Delta L_r = \Delta f_r / S_{\text{trim}}$. (5) If the trimming length is too large or minus, use a tuning set with a digital vernier caliper to tune the half-cell frequencies, as shown in Fig. 5. (6) Remeasure the individual half cells' frequencies of the tuned dumbbell; if their TM010 π frequencies and lengths meet the requirements, the final trimming lengths are determined, if not, redo the above steps.

In order to ensure the accuracy of the frequency measurements, maintaining a good electric contact between a

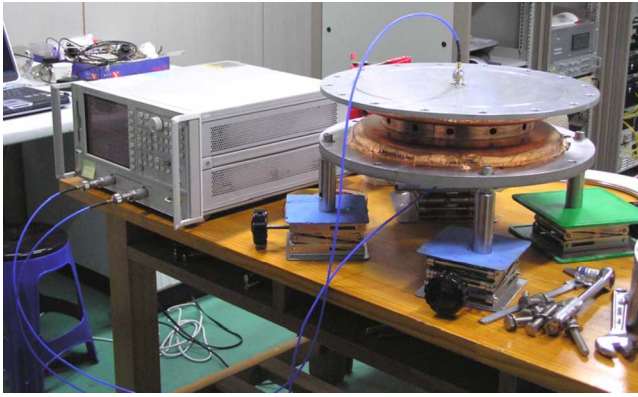


FIG. 6. (Color online) The setup to measure the PEFP dumbbell frequencies.

dumbbell and the used plates is very important, a loaded quality factor Q_L for the PEFP low-beta dumbbell measurements should be more than 200 during such frequency measurements. In order to avoid any effects by a room temperature change and the pressure of the fixtures, the testing was carried out at a constant temperature room. An aluminum tape was used to seal the dumbbell and the plates, but screw bolts and torque wrench were not used to adjust the pressure between the dumbbell and the plates during the testing.

According to this procedure, four PEFP low-beta dumbbells have been tuned successfully. Table II lists the data for a PEFP low-beta dumbbell before and after a tuning. Here we need to consider the shrinkage due to an electron beam welding at the equator, and because the tolerance control of a cavity length during a production and the dumbbell tuning are difficult tasks, the target length of a PEFP low-beta dumbbell cavity is specified as 91.280 ± 0.50 . During the tuning of the PEFP low-beta cavity listed in Table II, by using our tuning calculation and tuning method, one or two times can complete a dumbbell tuning.

V. CONCLUSION

Based on a two-coupled oscillator model and a cavity perturbation theory, a new formula to calculate the individual

TABLE II. The individual half-cell frequencies of a PEFP low-beta dumbbell before a tuning and after a tuning, and the trimming length at the equators of a tuned dumbbell.

Dumbbell state and trimming length	TM010 mode (MHz)
Target frequency	f_π 697.907
Target length (mm)	91.280 ± 0.50
Before tuning	$f_{l,\pi}$ 695.540
	$f_{r,\pi}$ 698.171
	K 1.76%
	η_{ff} 100.5%
After tuning	$f_{l,\pi}$ 697.075
	$f_{r,\pi}$ 697.719
	K 1.57%
	η_{ff} 12.3%
Trimming length (mm)	Left half cell 0.229
	Right half cell 0.040
Length after trimming (mm)	91.731

half-cell frequencies of a dumbbell or the individual cavity frequencies of a two-cavity coupling system has been developed and its performance has been confirmed by using a dumbbell simulation. This formula can be applied to any kind of rf cavities with electric, magnetic, or electromagnetic coupling, if a coupling hole between two coupling cavities is small compared to the wavelength. Compared to other calculation formulae, this formula simplifies the calculation process of the individual resonator frequencies of a coupling system considerably, and it can also improve the calculation precision than that of a normal calculation method. Another advantage of this new method is that we do not need to consider a coupling factor between two resonators during a testing for an individual resonator frequency of an oscillator. This measurement method can achieve a measurement of a dumbbell's individual half cells' frequencies, length, and field flatness at the same time. The developed formula has been successfully used to tune the PEFP dumbbells.

ACKNOWLEDGMENTS

The authors would like to thank P. Kneisel from JLab for the essential assistance in designing the frequency measurement and tuning sets. This work is supported by the 21C Frontier R&D program in Ministry of Science and Technology of the Korean Government.

- ¹J. R. Alonso, *Rev. Sci. Instrum.* **67**, 1308 (1996).
- ²M. Sawamura, R. Nagai, N. Kikuzawa, M. Sugimoto, N. Nishimori, and E. J. Minehara, *Rev. Sci. Instrum.* **70**, 3865 (1999).
- ³R. Gebel, O. Felden, and P. von Rossen, *Rev. Sci. Instrum.* **75**, 1860 (2004).
- ⁴J.-W. Kim, A. Goto, and Y. Yano, *Rev. Sci. Instrum.* **70**, 2293 (1999).
- ⁵S. H. Kim, M. Doleans, D. O. Jeon, and R. Sunlelin, *Nucl. Instrum. Methods Phys. Res. A* **492**, 1 (2002).
- ⁶R. Benaroya and K. W. Shepard, *Rev. Sci. Instrum.* **59**, 2100 (1988).
- ⁷S. An, H. Wang, and G. Wu, Proceedings of the LINAC 2004, Lübeck, Germany, August 2004, p. 815.
- ⁸S. An, Y. S. Cho, B. H. Choi, and J. H. Jang, *J. Korean Phys. Soc.* **50**, 1421 (2007).
- ⁹S. An, H. S. Kim, Y. S. Cho, and B. H. Choi, *J. Korean Phys. Soc.* **52**, 793 (2008).
- ¹⁰S. An, Y. S. Cho, and B. H. Choi, Proceedings of the APAC'07, Indore, January 2007, p. 564.
- ¹¹S. An, C. Gao, Y. S. Cho, and B. H. Choi, Proceedings of the PAC'07, Albuquerque, NM, June 2007, p. 2164.
- ¹²S. An, Y. S. Cho, and B. H. Choi, Proceedings of the APAC'07, Indore, January 2007, p. 506.
- ¹³H. Padamsee, J. Knobloch, and T. Hays, *RF Superconductivity for Accelerators* (Wiley, New York, 1998), p. 140.
- ¹⁴C. Yinghua, J. Sekutowicz, and W. Yixiang, Proceedings of the Fourth Workshop on RF Superconductivity, Tsukuba, Japan, 1990/DESY-M-89-11, August 1989.
- ¹⁵S. An, T. Yazhe, Z. Liping, Y.-m. Li, G. Changyi, and Y. S. Cho, Proceedings of the EPAC'08, Genoa, Italy, June 2008, p. 823.
- ¹⁶Los Alamos Accelerator Code Group, *Poisson/Superfish Reference Manual* (Los Alamos National Laboratory, Los Alamos, NM, 1987), p. LA-UR-87-126.
- ¹⁷CST MICROWAVE STUDIO, Version 5, Getting Started, *CST-Computer Simulation Technology*, 2003.
- ¹⁸H. A. Bethe, *Phys. Rev.* **66**, 163 (1944).
- ¹⁹E. L. Ginzton, *Microwave Measurements* (McGraw-Hill, New York, 1957), p. 448.
- ²⁰G. Ciovati, P. Kneisel, and J. Sekutowicz, *Method to adjust frequency and length of dumbbells to nominal values* (TJNAF, Newport News, VA, 2002), Paper No. JLab-TN-02-005-1.